

**Supporting Information:**

**Novel imino- and aryl-sulfonate based photoacid generators for the cationic ring-opening polymerization of  $\epsilon$ -Caprolactone**

Xabier Lopez de Pariza<sup>a</sup>, Erick Cordero Jara<sup>a,c</sup>, Nicolas Zivic<sup>a</sup>, Fernando Ruipérez<sup>a</sup>, Timothy E. Long<sup>b</sup>, Haritz Sardon<sup>a\*</sup>

<sup>a</sup>*POLYMAT and Departamento de Química Aplicada, Facultad de Ciencias Químicas, University of the Basque Country UPV/EHU, Joxe Mari Korta zentroa, Tolosa Hiribidea 72, Donostia-San Sebastián 20018, Spain.*

<sup>b</sup>*Arizona State University, School of Molecular Science and Biodesign Center for Sustainable Macromolecular Materials and Manufacturing, Tempe, Arizona 85281, United States.*

<sup>c</sup>*School of Microbiology, Universidad de Ciencias Médicas (UCIMED), San José, Costa Rica.*

## Table of contents

1. Experimental procedures .....	3
2. Synthetic procedures .....	4
3. Supplementary figures .....	13
4. Supplementary methods.....	31
5. References.....	32

## 1. Experimental procedures

**Photolysis study of Photoacid generators by  $^1\text{H}$  NMR.** In a 12 mL vial, a 0.25 M solution of photoacid was dissolved in  $\text{DMSO-d}_6$  and irradiated over time using a LED centered at 365 nm (Hamamatsu,  $60 \text{ mW}\cdot\text{cm}^{-2}$ ). The intensity of the UV output was calibrated using an external radiometer. The photolysis of the photoacid was tracked by the disappearance of the methyl p-toluenesulfonate protons of the PAGs (2.42 ppm) and the following appearance of the methyl protons of the p-toluenesulfonic acid (2.29 ppm). For methanesulfonate containing PAGs, the disappearance of the methanesulfonate protons (3.33 ppm) was tracked followed by the appearance of the methyl protons of methanesulfonic acid (3.05 ppm) the photolysis was carried out in  $\text{CDCl}_3$  due to overlapping of the signal with the solvent peak. In the case of the trifluoromethane sulfonate containing PAGs,  $^{19}\text{F}$  NMR was used to follow the photolysis by the disappearance of the trifluoromethane sulfonate signal (-71.0 and -72.5 ppm respectively) and the subsequent trifluoro sulfonate acid  $\text{CF}_3$  band (-78.1 ppm).

**Photolysis study of Photoacid generators by UV-VIS spectroscopy.** PAG solutions ( $1\cdot 10^{-4}$ – $4\cdot 10^{-3}$  M) were dissolved in acetonitrile and irradiated with a 365 nm centered LED (Hamamatsu,  $60 \text{ mW cm}^{-2}$ ). The intensity of the light was measured by an external radiometer.

### **Typical procedure for ring-opening polymerization of $\epsilon$ -caprolactone at room temperature by using Oxime-sulfonate and Aryl-sulfonate PAGs**

In a 5 mL vial equipped with a magnetic stirrer,  $\epsilon$ -caprolactone ( $\epsilon$ -Cl) (1.5 mmol), was dissolved in 1.5 mL of  $\text{CDCl}_3$  ( $[\epsilon\text{-Cl}]_0 = 1.0 \text{ M}$ ) together with the photoacid generators (PAG) and the Initiator (BnOH) ( $[\text{BnOH}]:[\text{PAG}] = [1]:[1]$ ) under atmospheric conditions. The solution was stirred at room temperature and irradiated with a LED centered at 365 nm (Hamamatsu,  $60 \text{ mW}\cdot\text{cm}^{-2}$ ). The samples were quenched with Amberlyst A21 basic resin and monomer consumption was tracked by  $^1\text{H}$  NMR following the disappearance of the monomer methylene signal (4.23 ppm) and the subsequent appearance of the polymer methylene signals at 4.06 and 3.62 ppm.  $^1\text{H}$  NMR (300 MHz,  $\text{CDCl}_3$ )  $\delta$ (ppm): 5.10 ( $\text{ArCH}_2-$ ), 4.05 ( $-\text{CH}_2\text{O}-$ ), 3.63 ( $-\text{CH}_2\text{OH}$ ), 2.29 ( $-\text{OCOCH}_2-$ ), 1.64 ( $-\text{CH}_2\text{CH}_2\text{CH}_2\text{O}-$ ), 1.37 ( $-\text{CH}_2\text{CH}_2\text{CH}_2\text{CH}_2\text{CH}_2-$ ).

### **Typical procedure for ring-opening polymerization of $\epsilon$ -caprolactone at different temperatures by using Oxime-sulfonate and Aryl-sulfonate PAGs**

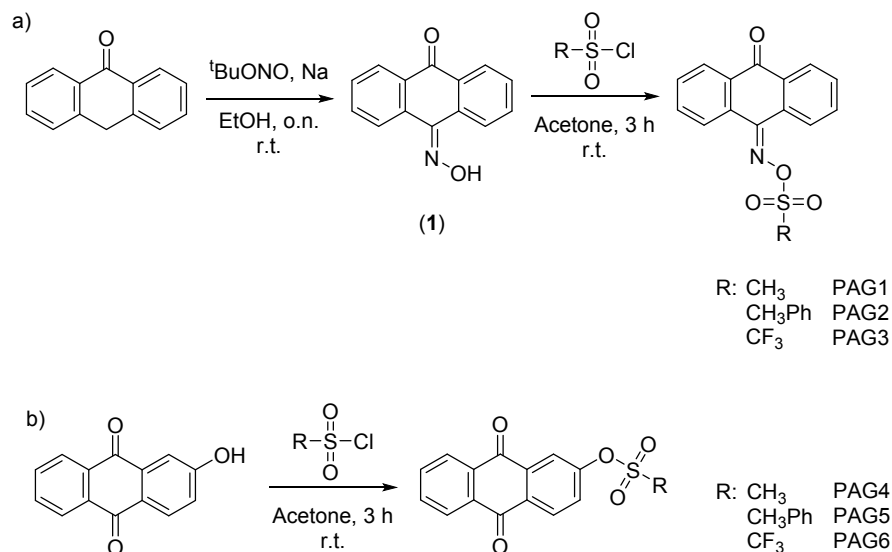
In a 5 mL vial equipped with a magnetic stirrer,  $\epsilon$ -caprolactone ( $\epsilon$ -Cl) (1.5 mmol, 100 eq.), was mixed with the photoacid generator (PAG) (0.075 mmol, 5 eq.) and benzyl alcohol (0.15 mmol, 10 eq.) under atmospheric conditions in an oil bath. The solution was stirred at the desired temperature while irradiating with a LED centered at 365 nm (Hamamatsu,  $60 \text{ mW}\cdot\text{cm}^{-2}$ ). Samples were acquired at different times and quenched with Amberlyst A21 basic resin for conversion analysis. Monomer consumption was tracked by  $^1\text{H}$  NMR following the disappearance of the monomer methylene signal (4.23 ppm) and the subsequent appearance of the polymer methylene signals at 4.06 and 3.62 ppm.

### **Typical procedure for crosslinked film formation of $\epsilon$ -caprolactone using BCY as crosslinker**

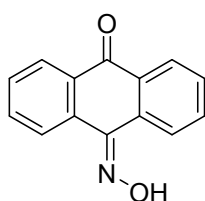
In a 12 mL vial,  $\epsilon$ -caprolactone ( $\epsilon$ -Cl) (1026 mg, 9 mmol, 100 eq.), BCY (203 mg, 0.9 mmol, 10 eq.) and PCL-900 triol (270 mg, 0.3 mmol 3.3 eq.) were mixed together with PAG3 (160 mg, 0.45 mmol, 5 eq.). From this mixture aliquots of 150  $\mu\text{L}$  were transferred into silicone dishes with a diameter of 1 cm and irradiated over 7 hours with a LED light centered at 365 nm (Hamamatsu,  $60 \text{ mW}\cdot\text{cm}^{-2}$ ). Afterwards, the plates were cured for 72 h in the darkness.

## 2. Synthetic procedures

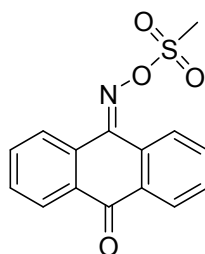
### Synthesis of the PAGs:



Scheme S1: Synthetic route of the studied PAGs.



**10-(hydroxyimino)anthracen-9(10H)-one (1):** T-butyl nitrite (7.96 g, 77.2 mmol, 1.5 eq.) was added to a stirring solution of sodium (1.66 g, 72.1 mmol, 1.4 eq.) in ethanol (195 mL) under nitrogen atmosphere. To the resulting solution, anthrone (10.00 g, 51.48 mmol, 1 eq.) was added. The reaction was stirred overnight and then poured into 60 mL of ice-cold water. After treating the solution with 15 mL of 1 M HCl the resulting solid was collected by filtration, washed with water and dried under reduced pressure. The residue was further washed with hexane and again dried under reduced pressure. The pure product was obtained as a white-yellowish powder with a moderate yield (3.54 g, 31 %) after purification by flash column chromatography using DCM as eluent. Further characterization was consistent with previously reported literature.<sup>1</sup>  **$^1\text{H-NMR}$  (300 MHz, DMSO- $d_6$ )  $\delta$  (ppm):** 13.25 (s, 1H), 9.12 (d, 1H), 8.31 (d, 1H), 8.30-8.13 (m, 2H), 7.92 – 7.60 (m, 4H). **FTIR (ATR):** 3248 (-O-H), 1646 (-C=O), 1589 (-C=C-), 1463 (-C=N-)  $\text{cm}^{-1}$ .



**10-(((methylsulfonyl)oxy)imino)anthracen-9(10H)-one (PAG1):** To an ice-cooled solution of **1** (0.50 g, 2.24 mmol, 1 eq.) and methanesulfonyl chloride (0.26 g, 2.24 mmol, 1 eq.) in anhydrous acetone (50 mL), triethylamine (0.34 mL, 0.25 g, 2.46 mmol, 1.1 eq.) was added under  $\text{N}_2$  atmosphere. The reaction mixture was then stirred at room temperature over 3 h. Afterwards, 100 mL of  $\text{H}_2\text{O}$  were added and the formed precipitate filtrated: After washing the solid several times with  $\text{H}_2\text{O}$ , the pure product was obtained as a white-yellowish solid (0.60 g, 90 %).  $T_d$ : 188 °C from TGA analysis.  **$^1\text{H-NMR}$  (300 MHz, DMSO- $d_6$ )  $\delta$  (ppm):** 8.60 – 8.57 (d, 1H), 8.27 (m, 2H), 8.20-8.14 (d, 1H), 7.95 – 7.75 (m, 5H), 3.61 (s, 3H).  **$^{13}\text{C NMR}$  (300 MHz, DMSO- $d_6$ ,  $\delta$  (ppm):** 182.0, 150.2, 134.5, 134.1, 134.0, 133.7, 133.0, 131.9, 131.2, 130.7, 127.5, 126.7, 125.5, 36.7. **FTIR (ATR):** 1662 (-C=O), 1598, 1585 (-C=C-), 1460 (-C=N-), 1187 (S=O)  $\text{cm}^{-1}$ . **HRMS (ESI):**  $m/z$  calc. for  $\text{C}_{15}\text{H}_{12}\text{NO}_4\text{S}$ : 302.0487 [M + H]<sup>+</sup>; found: 302.0493.

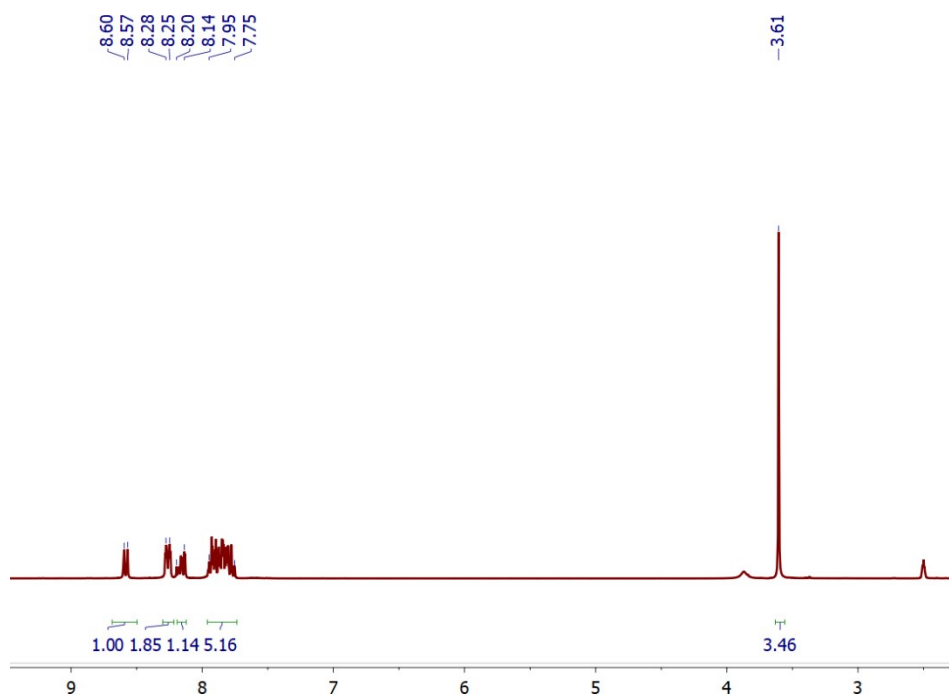


Figure S1:  $^1\text{H}$  NMR spectra of PAG1 in  $\text{DMSO-d}_6$ .

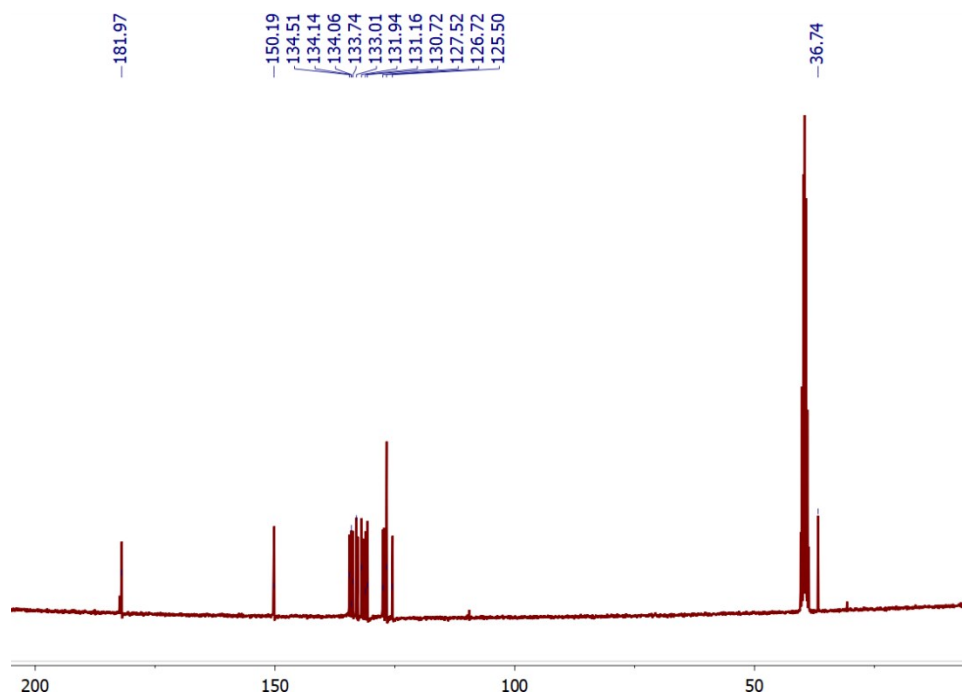
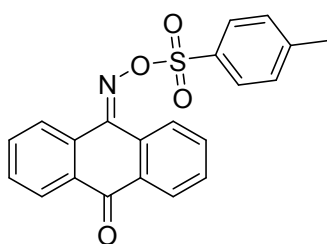


Figure S2:  $^{13}\text{C}$  NMR spectra of PAG1 in  $\text{DMSO-d}_6$ .



**10-((tosyloxy)imino)anthracen-9(10H)-one (PAG2):** To an ice-cooled solution of **1** (0.50 g, 2.24 mmol, 1 eq.) and p-toluenesulfonyl chloride (0.47 g, 2.24 mmol, 1.1 eq.) in anhydrous acetone (50 mL) was added triethylamine (0.34 mL, 0.25 g, 2.46 mmol, 1.1 eq.) under  $\text{N}_2$  atmosphere. The reaction mixture was then stirred at room temperature over 3 h. Afterwards, 100 mL of  $\text{H}_2\text{O}$  were added and the formed precipitate filtrated: After washing the solid several times with  $\text{H}_2\text{O}$ , the pure product was obtained as a white-yellowish

solid (0.71 g, 84 %).  $T_d$ : 204 °C from TGA analysis.  $^1\text{H NMR}$  (300 MHz,  $\text{DMSO-d}_6$ ,  $\delta$  (ppm)): 8.59 (d, 1H), 8.27 (d, 1H), 8.14 (d, 1H), 8.04 (d, 2H), 7.99 – 7.73 (m, 5H), 7.55 (d, 2H), 2.42 (s, 3H).  $^{13}\text{C NMR}$  (300 MHz,  $\text{DMSO-d}_6$ ,  $\delta$  (ppm)): 181.8, 150.3, 146.3, 134.2, 133.8, 132.9, 132.0, 131.8, 131.1, 131.0, 130.7, 130.3, 128.9, 127.6, 127.2, 126.8, 124.9, 114.5, 21.3. **FTIR (ATR)**: 1664 (-C=O), 1585 (-C=C-), 1442 (-C=N-), 1193, 1169, 1095 (S=O)  $\text{cm}^{-1}$ . **HRMS (ESI)**:  $m/z$  calc. for  $\text{C}_{21}\text{H}_{16}\text{NO}_4\text{S}$ : 378.0800  $[\text{M} + \text{H}]^+$ ; found: 378.0804.

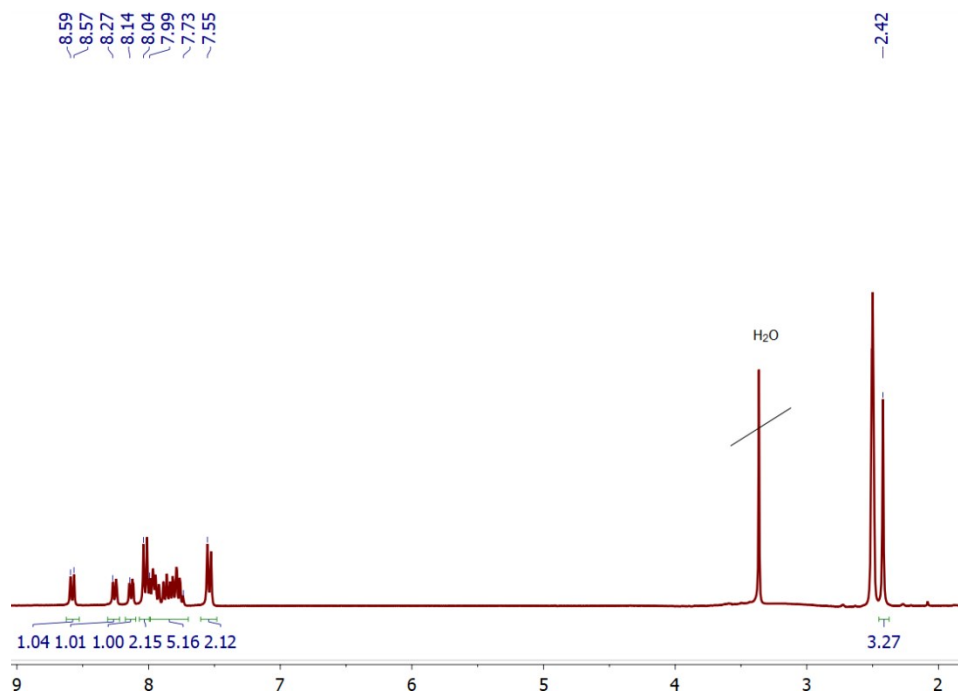


Figure S3:  $^1\text{H NMR}$  spectra of PAG2 in  $\text{DMSO-d}_6$ .

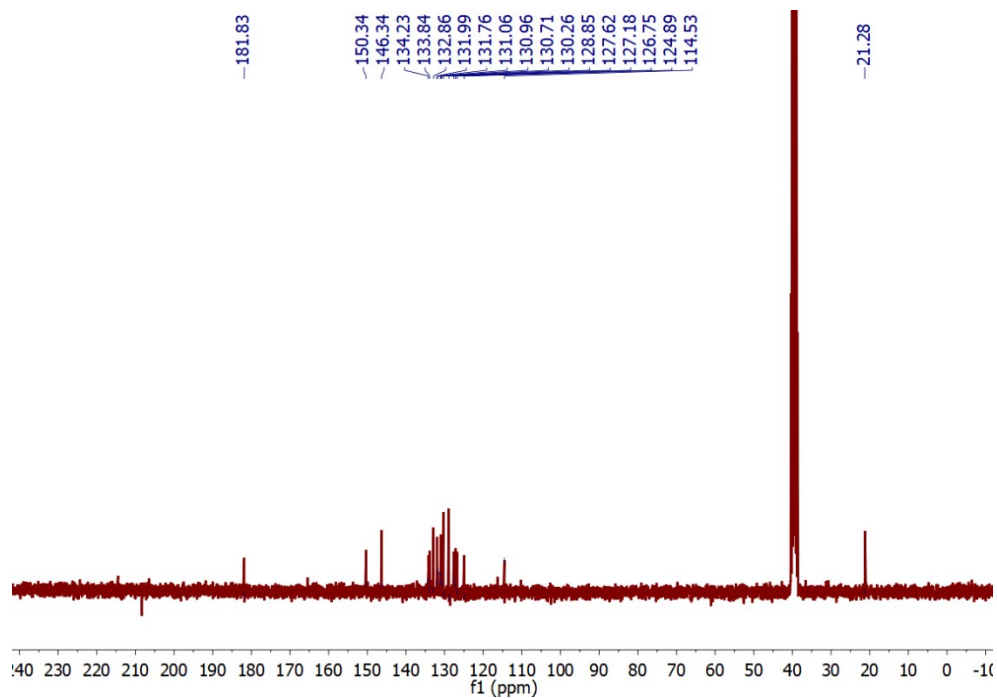
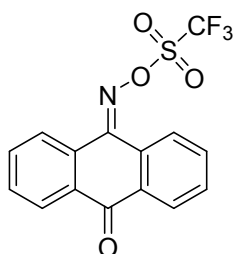


Figure S4:  $^{13}\text{C NMR}$  spectra of PAG2 in  $\text{DMSO-d}_6$ .



**10-(((trifluoromethyl)sulfonyl)oxy)imino)anthracen-9(10H)-one (PAG3)**: To an ice-cooled solution of 1 (0.50 g, 2.24 mmol, 1 eq.) and

trifluorosulfonyl chloride (0.26 mL, 0.42 g, 2.46 mmol, 1.1 eq.) in anhydrous acetone (50 mL) was added triethylamine (0.343 mL, 0.25 g, 2.46 mmol, 1.1 eq.) under N<sub>2</sub> atmosphere. The reaction mixture was then stirred at room temperature over 3 h. Afterwards, 100 mL of H<sub>2</sub>O were added and the formed precipitate filtrated: After washing the solid several times with H<sub>2</sub>O, the pure product was obtained as a white-yellowish solid (0.61 g, 77 %). T<sub>d</sub>: 167 °C from TGA analysis. **<sup>1</sup>H NMR (300 MHz, CDCl<sub>3</sub>, δ (ppm))**: 8.52 (m, 1H), 8.42 (m, 1H), 8.29 (m, 1H), 8.19 (m, 1H), 7.80 (m, 2H), 7.73 (m, 2H). **<sup>13</sup>C NMR (300 MHz, DMSO-d<sub>6</sub>, δ (ppm))**: 182.4, 154.3, 134.3, 134.1, 133.7, 133.3, 132.9, 132.3, 131.5, 128.6, 127.7, 127.4, 125.8, 118.95 (q, J = 322.5 Hz). **<sup>19</sup>F NMR (300 MHz, DMSO-d<sub>6</sub>, δ (ppm))**: 71.0. **FTIR (ATR)**: 1670 (-C=O), 1585 (-C=C-), 1423 (-C=N-), 1197, 1130 (S=O) cm<sup>-1</sup>. **HRMS (ESI)**: m/z calc. for C<sub>15</sub>H<sub>8</sub>F<sub>3</sub>NO<sub>4</sub>S: 356.0204 [M + H]<sup>+</sup>; found: 356.0202.

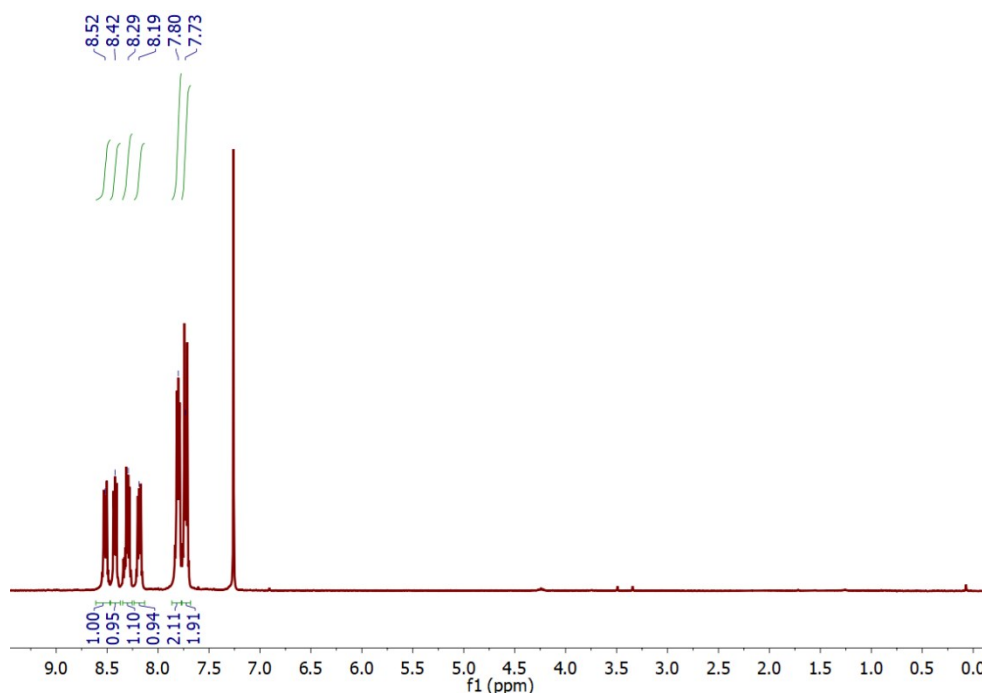


Figure S5: <sup>1</sup>H NMR spectra of PAG3 in DMSO-d<sub>6</sub>.

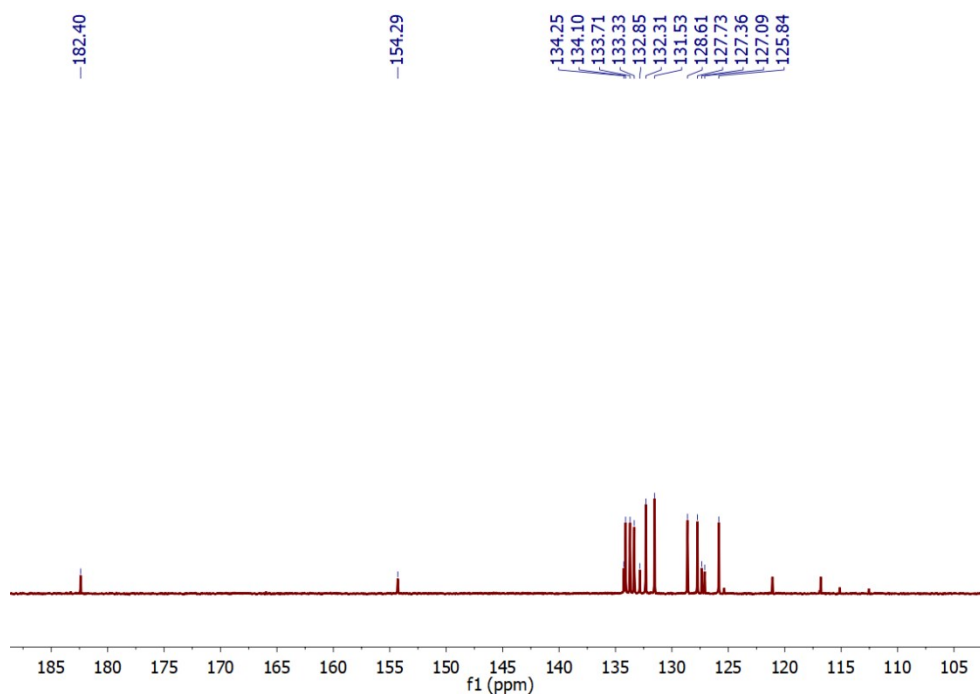


Figure S6:  $^{13}\text{C}$  NMR spectra of PAG3 in  $\text{DMSO-d}_6$ .

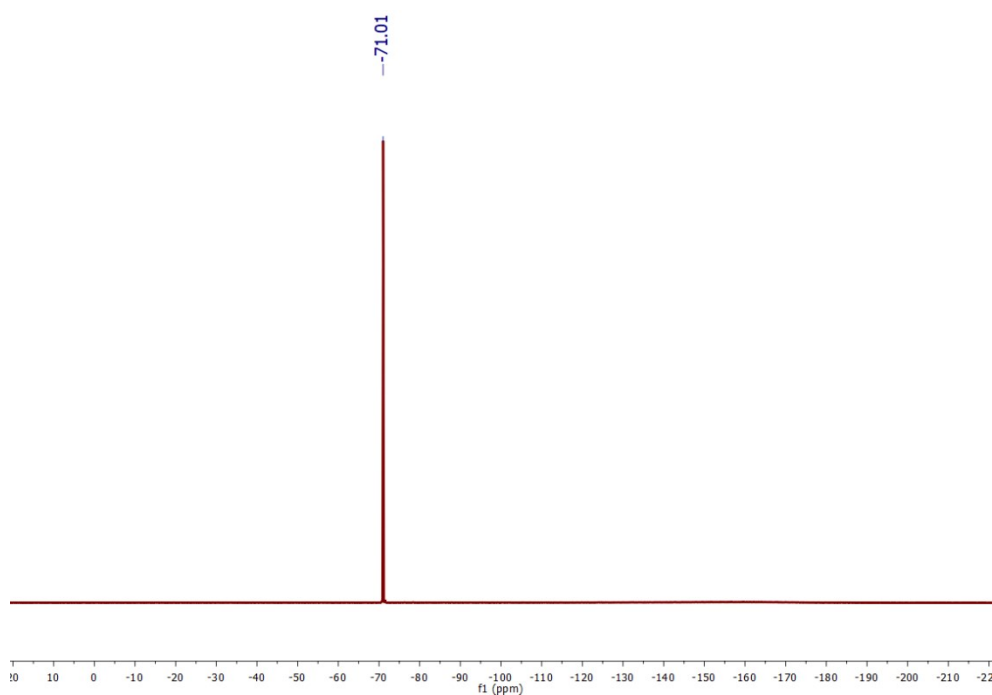
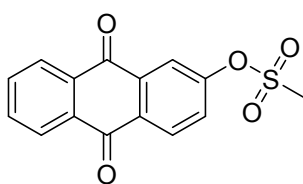


Figure S7:  $^{19}\text{F}$  NMR spectra of PAG3 in  $\text{DMSO-d}_6$ .



**9,10-dioxo-9,10-dihydroanthracen-2-yl methanesulfonate (PAG4):**

To an ice-cooled solution of 2-Hydroxyanthraquinone (0.50 g, 2.23 mmol, 1 eq.) and methanesulfonyl chloride (0.181 mL, 0.27 g, 2.34 mmol, 1.05 eq.) in anhydrous acetone (50 mL) was added triethylamine (0.326 mL, 0.24 g, 2.34 mmol, 1.05 eq.) under  $\text{N}_2$  atmosphere. The reaction mixture was then stirred at room temperature over 3 h. Afterwards, 100 mL of  $\text{H}_2\text{O}$  were added and the formed precipitate filtrated: After washing the solid several



times with H<sub>2</sub>O, the pure product was obtained as a green-brownish solid (0.61 g, 90 %). T<sub>d</sub>: 217 °C from TGA analysis. <sup>1</sup>H NMR (300 MHz, CDCl<sub>3</sub>, δ (ppm)): 8.41 (d, 1H), 8.31 (m, 2H), 8.15 (d, 1H), 7.83 (m, 2H), 7.72 (d, 1H), 3.28 (s, 3H). <sup>13</sup>C NMR (300 MHz, DMSO-d<sub>6</sub>, δ (ppm)): 181.5, 181.5, 153.0, 135.1, 134.8, 134.7, 133.0, 132.9, 131.7, 129.7, 128.0, 126.9, 119.7, 37.9. FTIR (ATR): 1673 (-C=O), 1587 (-C=C-), 1177, 1036 (S=O) cm<sup>-1</sup>. HRMS (ESI): m/z calc. for C<sub>15</sub>H<sub>11</sub>O<sub>5</sub>S: 303.0327 [M + H]<sup>+</sup>; found: 303.0332.

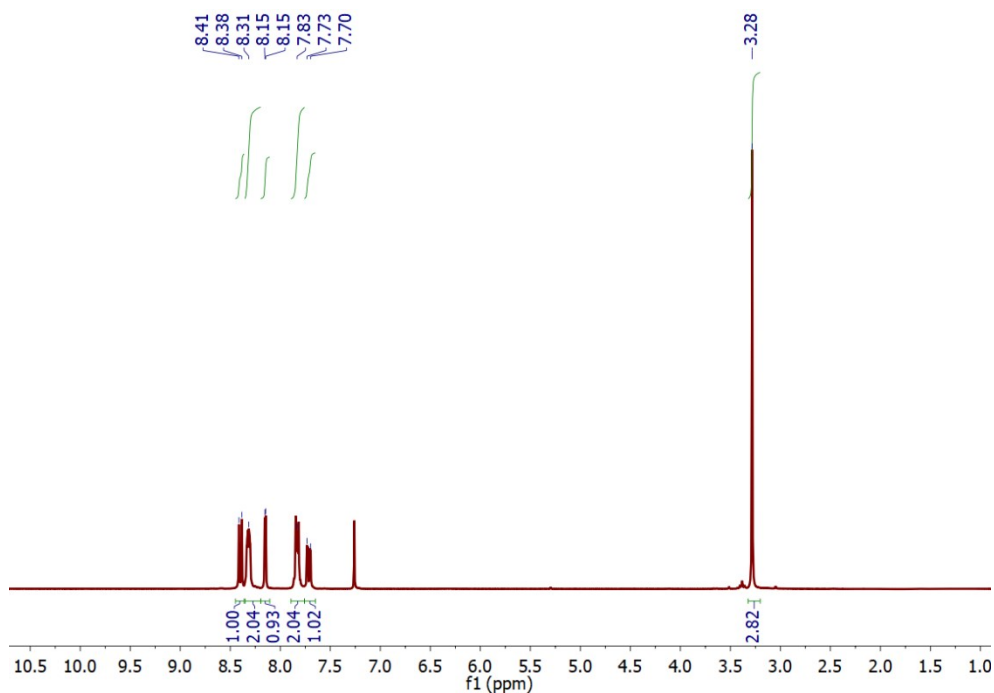


Figure S8: <sup>1</sup>H NMR spectra of PAG4 in CDCl<sub>3</sub>.

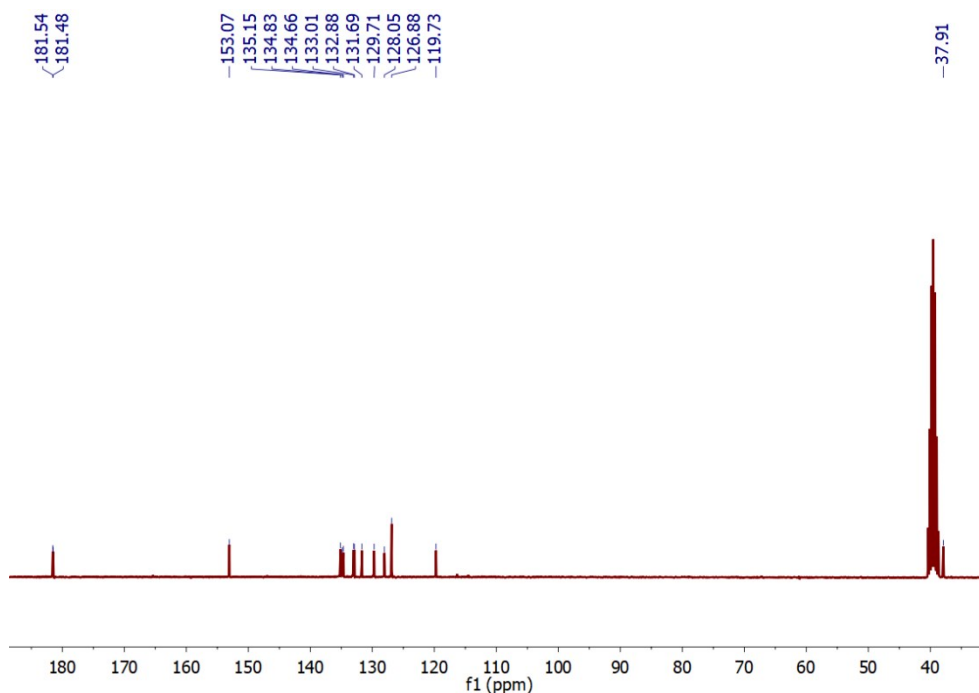
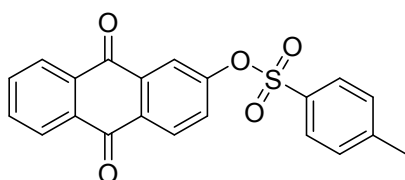


Figure S9: <sup>13</sup>C NMR spectra of PAG4 in DMSO-d<sub>6</sub>.



**9,10-dioxo-9,10-dihydroanthracen-2-yl 4-methylbenzene sulfonate (PAG5):** To an ice-cooled solution of 2-

Hydroxyanthraquinone (0.50 g, 2.23 mmol, 1 eq.) and p-toluenesulfonyl chloride (0.45 g, 2.34 mmol, 1.05 eq.) in anhydrous acetone (50 mL) was added triethylamine (0.326 mL, 0.24 g, 2.34 mmol, 1.05 eq.) under N<sub>2</sub> atmosphere. The reaction mixture was then stirred at room temperature over 3 h. Afterwards, 100 mL of H<sub>2</sub>O were added and the formed precipitate filtrated: After washing the solid several times with H<sub>2</sub>O, the pure product was obtained as a greenish solid (0.80 g, 95 %). T<sub>d</sub>: 197 °C from TGA analysis. **<sup>1</sup>H NMR (300 MHz, CDCl<sub>3</sub>, δ (ppm))**: 8.25-8.18 (m, 3H), 7.94 (m, 2H), 7.85 (d, 2H), 7.83 (m, 2H), 7.77 (d, 1H), 7.61-7.57 (m, 1H), 7.50 (d, 2H), 2.43 (s, 3H). **<sup>13</sup>C NMR (300 MHz, DMSO-d<sub>6</sub>, δ (ppm))**: 181.1, 152.7, 146.2, 135.0, 134.7, 134.5, 132.8, 132.8, 131.7, 131.0, 130.4, 129.6, 128.3, 127.8, 126.8, 119.4, 21.1. **FTIR (ATR)**: 1670 (-C=O), 1589, (-C=C-), 1184, 1172, 1087 (S=O) cm<sup>-1</sup>. **HRMS (ESI)**: m/z calc. for C<sub>21</sub>H<sub>15</sub>O<sub>5</sub>S: 379.0640 [M + H]<sup>+</sup>; found: 379.0636.

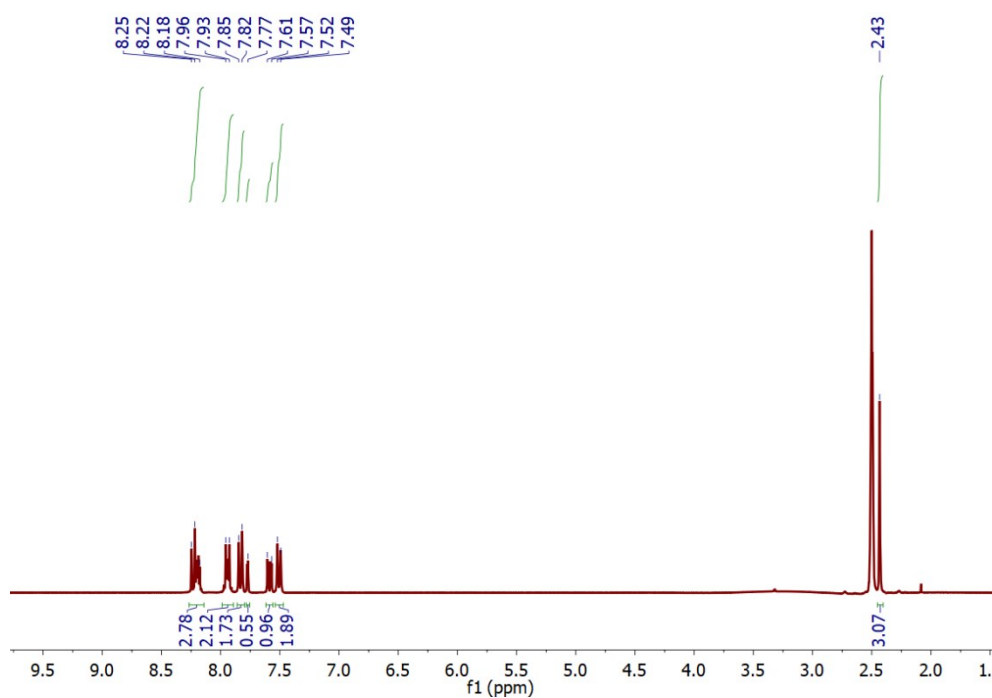


Figure S10: <sup>1</sup>H NMR spectra of PAG5 in DMSO-d<sub>6</sub>.

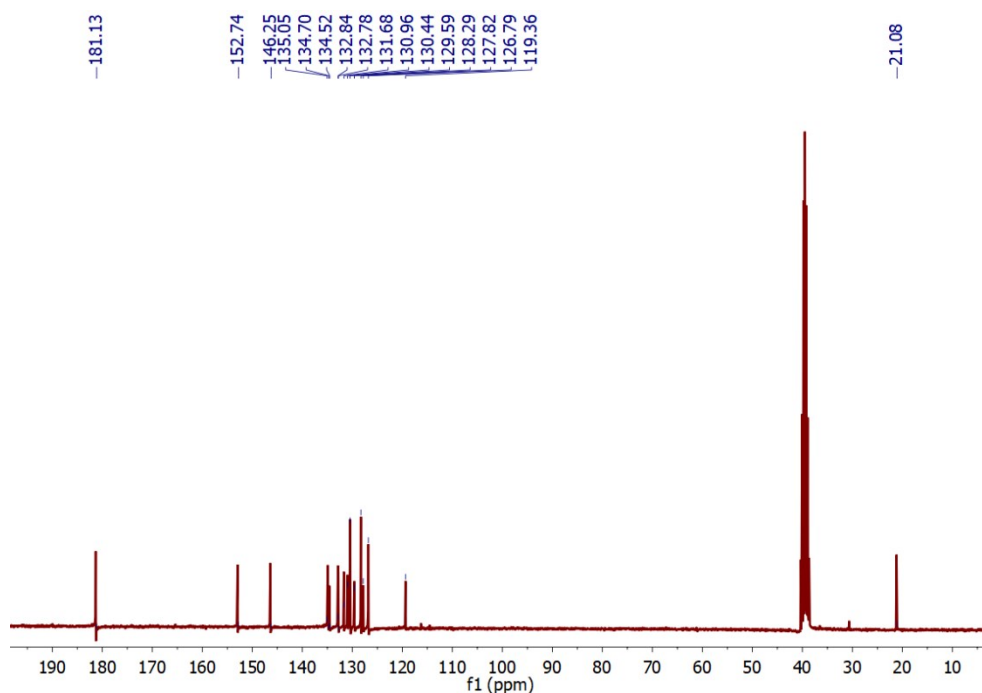
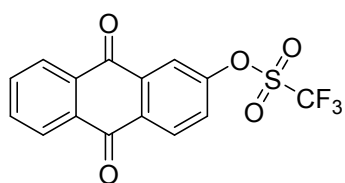


Figure S11:  $^{13}\text{C}$  NMR spectra of PAG5 in  $\text{DMSO-d}_6$ .



**9,10-dioxo-9,10-dihydroanthracen-2-yltrifluoromethane sulfonate (PAG6):**

To an ice-cooled solution of 2-Hydroxyanthraquinone (0.50 g, 2.23 mmol, 1 eq.) and trifluorosulfonyl chloride (0.25 mL, 0.39 g, 2.34 mmol, 1.05 eq.) in anhydrous acetone (50 mL) was added triethylamine (0.326 mL, 0.24 g, 2.34 mmol, 1.05 eq.) under  $\text{N}_2$  atmosphere. The reaction mixture was then stirred at room temperature over 3 h. Afterwards, 100 mL of  $\text{H}_2\text{O}$  were added and the formed precipitate filtrated: After washing the solid several times with  $\text{H}_2\text{O}$ , the pure product was obtained as a purple solid (0.67 g, 85 %).  $T_d$ : 160 °C from TGA analysis.  $^1\text{H}$  NMR (300 MHz,  $\text{DMSO-d}_6$ ,  $\delta$  (ppm): 8.35 (d, 1H), 8.18 (m, 2H), 8.10 (d, 1H), 8.00 (dd, 1H), 7.92 (m, 2H).  $^{13}\text{C}$  NMR (300 MHz,  $\text{DMSO-d}_6$ ,  $\delta$  (ppm): 181.3, 181.1, 152.8, 135.5, 135.0, 134.9, 133.0, 132.9, 130.3, 127.3, 127.0, 119.2, 118.32 (q,  $J = 320.9$  Hz).  $^{19}\text{F}$  NMR (300 MHz,  $\text{DMSO-d}_6$ ,  $\delta$  (ppm): 72.6. FTIR (ATR): 1675 (-C=O), 1589, (-C=C-), 1131, 1089, 1036 (S=O). HRMS (ESI):  $m/z$  calc. for  $\text{C}_{15}\text{H}_8\text{FO}_5\text{S}$ : 357.0045 [M + H] $^+$ ; found: 357.0043.

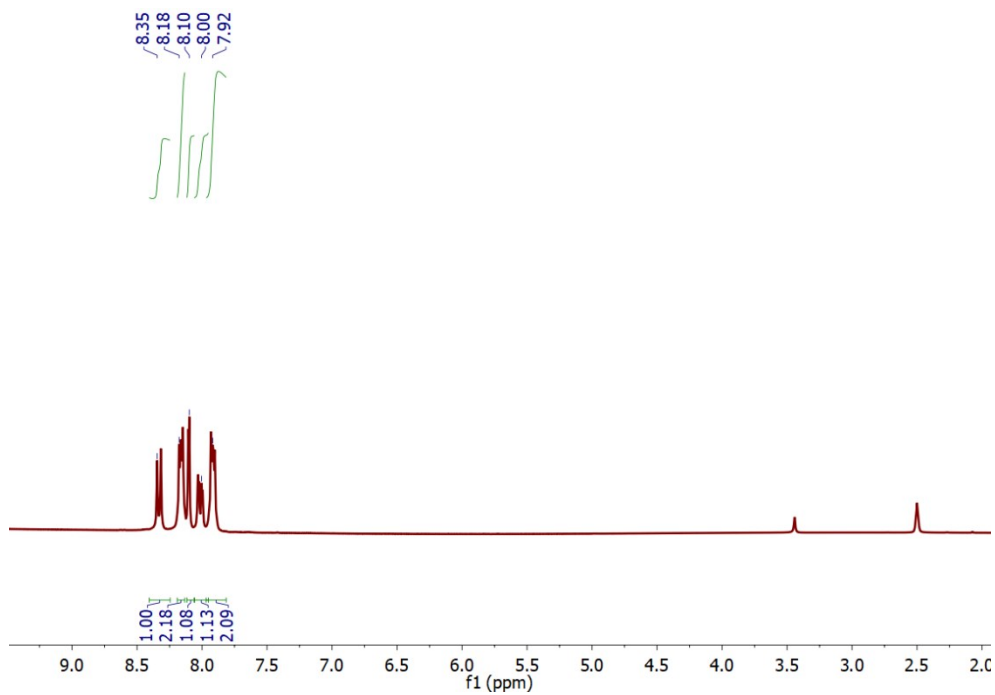


Figure S12:  $^1\text{H}$  NMR spectra of PAG6 in  $\text{DMSO-d}_6$ .

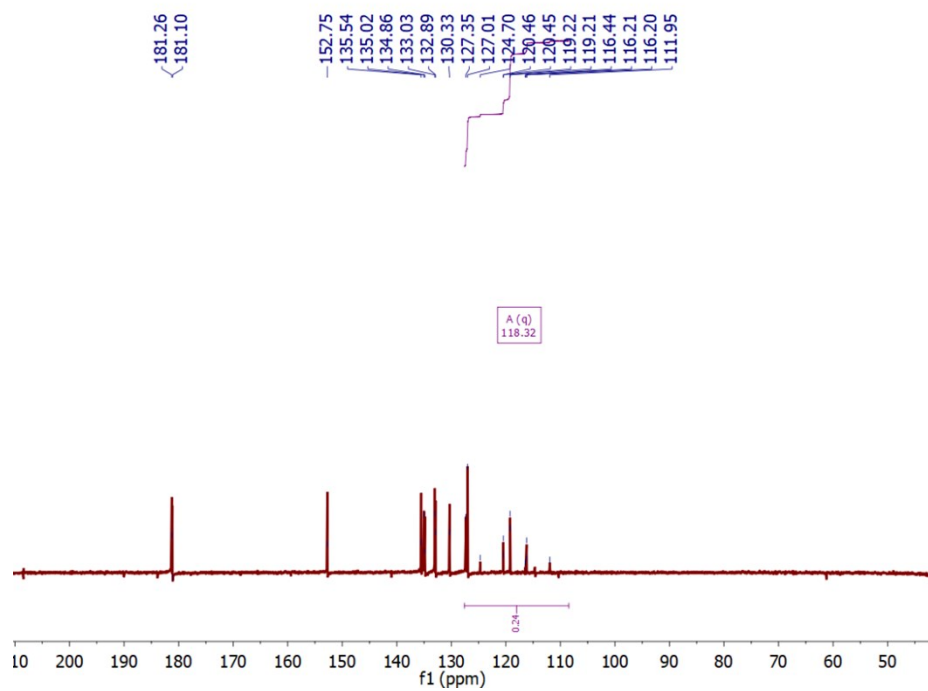


Figure S13:  $^{13}\text{C}$  NMR spectra of PAG6 in  $\text{DMSO-d}_6$ .

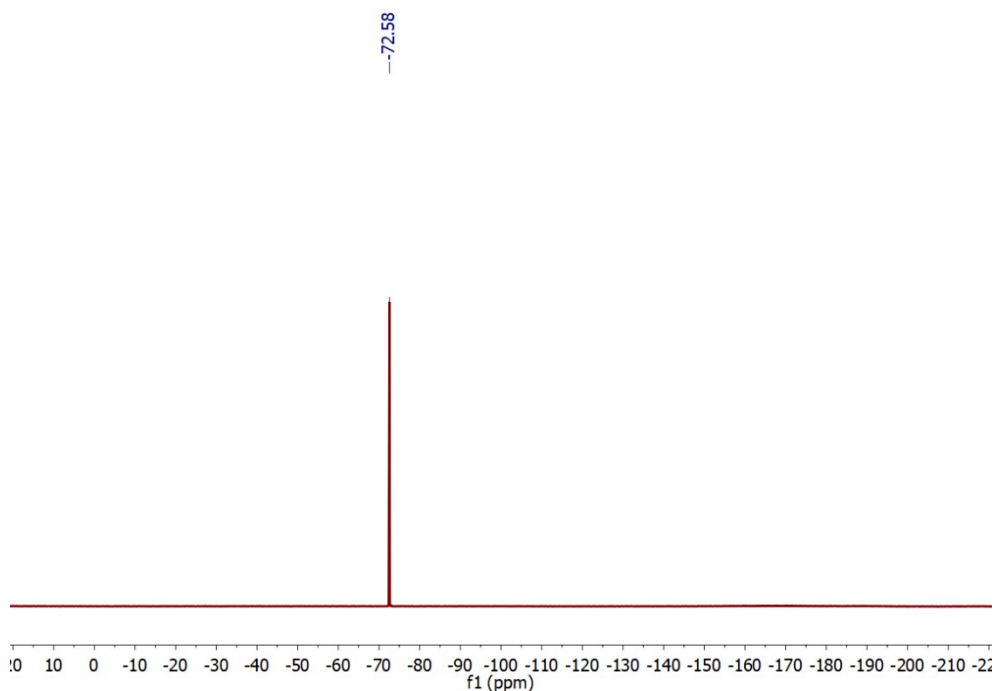
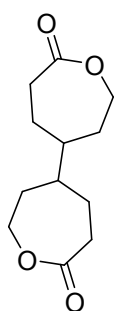


Figure S14: <sup>19</sup>F NMR spectra of PAG6 in DMSO-d<sub>6</sub>.

#### Synthesis of bis-( $\epsilon$ -caprolactone-4-yl) (BCY)



**bis-( $\epsilon$ -caprolactone-4-yl) (BCY):** BCY was synthesized by Baeyer-Villiger oxidation of 1,1'-bi(cyclohexyl)-4,4'-dione following the procedure reported elsewhere.<sup>2</sup> For that, 30 g of m-CPBA (173 mmol, 2.8 eq.) were dissolved in 250 mL of DCM and cooled to 10 °C before the aqueous phase was removed by decantation. To this solution, a solution of 12 g of 1,1-bi(cyclohexyl)-4,4-dione (61 mmol, 1 eq.) was added dropwise over 1.5 h keeping the bath temperature at 10 °C, then stirred at room temperature overnight. Afterwards, the mixture was extracted with sat. NaHCO<sub>3</sub> (3X400 mL) and saturated brine (3X400 mL). The organic phases were combined, dried over MgSO<sub>4</sub> and the solvent removed to afford a white solid. The

crude product was purified twice by crystallization in acetone to afford the pure product as a crystalline solid (11 g, 79 %). <sup>1</sup>H NMR (300 MHz, CDCl<sub>3</sub>)  $\delta$ (ppm): 4.30 (m, 2H), 4.15 (m, 2H), 2.65 (m, 4H), 1.91-1.79 (m, 4H), 1.63 (m, 4H), 1.47 (m 2H).

### 3. Supplementary figures

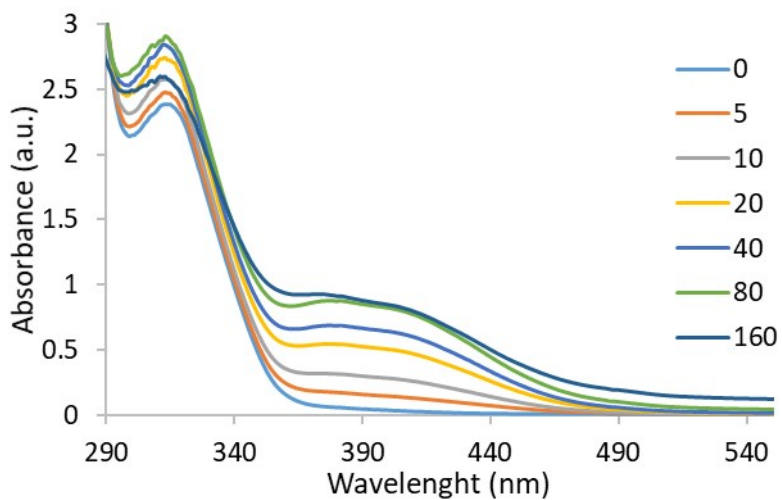


Figure S15: Light absorption spectra of PAG1 ( $c = 1 \cdot 10^{-4}$  M in ACN) irradiated at different times with a LED source centered at 365 nm (Hamamatsu,  $60 \text{ mW} \cdot \text{cm}^{-2}$ ). Irradiation times are shown in seconds.

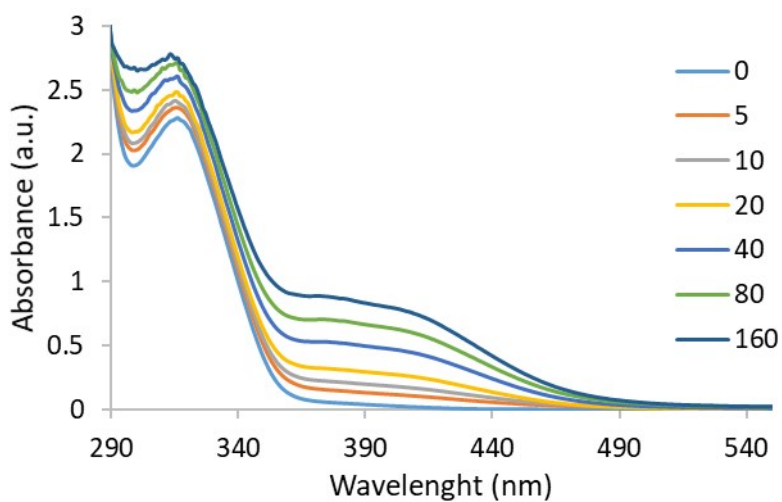


Figure S16: Light absorption spectra of PAG2 ( $c = 1 \cdot 10^{-4}$  M in ACN) irradiated at different times with a LED source centered at 365 nm (Hamamatsu,  $60 \text{ mW} \cdot \text{cm}^{-2}$ ). Irradiation times are shown in seconds.

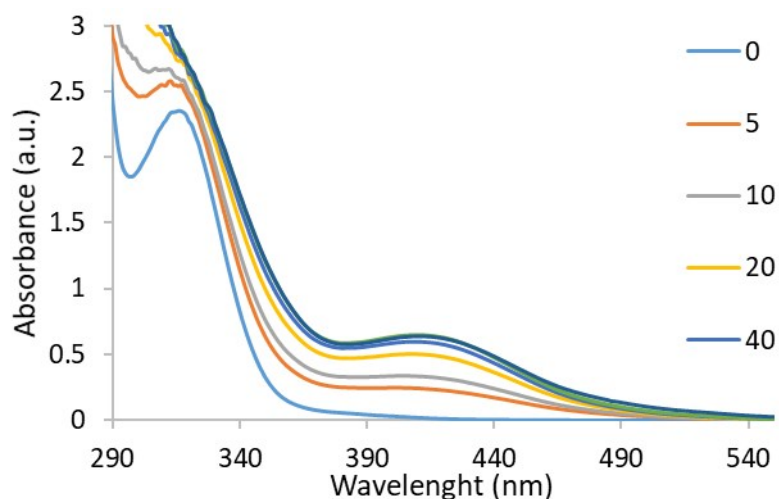


Figure S17: Light absorption spectra of PAG3 ( $c = 1 \cdot 10^{-4}$  M in ACN) irradiated at different times with a LED source centered at 365 nm (Hamamatsu,  $60 \text{ mW} \cdot \text{cm}^{-2}$ ). Irradiation times are shown in seconds.

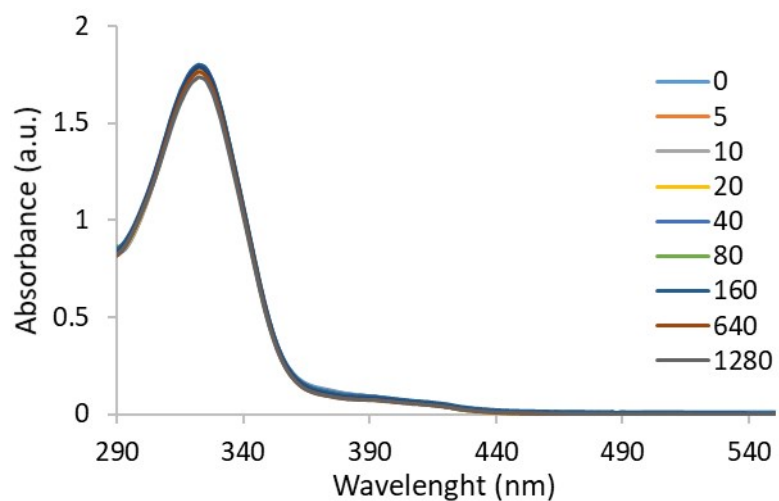


Figure S18: Light absorption spectra of PAG4 ( $c = 4 \cdot 10^{-4}$  M in ACN) irradiated at different times with a LED source centered at 365 nm (Hamamatsu,  $60 \text{ mW} \cdot \text{cm}^{-2}$ ). Irradiation times are shown in seconds.

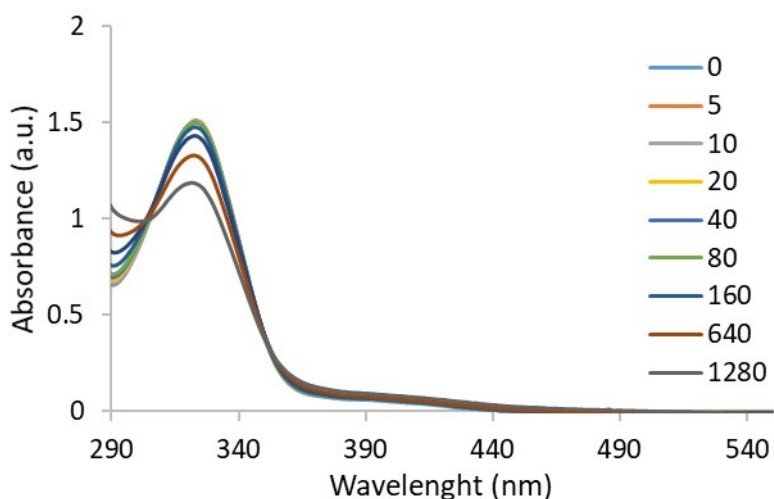


Figure S19: Light absorption spectra of PAG5 ( $c = 1 \cdot 10^{-4}$  M in ACN) irradiated at different times with a LED source centered at 365 nm (Hamamatsu,  $60 \text{ mW} \cdot \text{cm}^{-2}$ ). Irradiation times are shown in seconds.

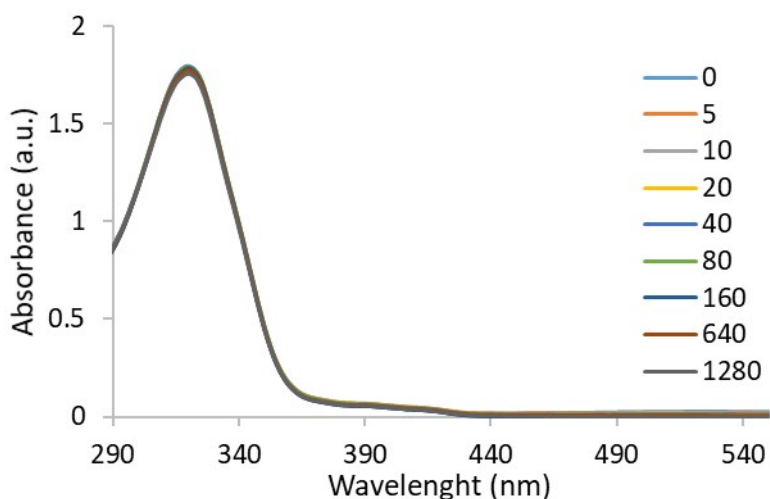


Figure S20: Light absorption spectra of PAG6 ( $c = 4 \cdot 10^{-4}$  M in ACN) irradiated at different times with a LED source centered at 365 nm (Hamamatsu,  $60 \text{ mW} \cdot \text{cm}^{-2}$ ). Irradiation times are shown in seconds.

Table S1: Thermal and photophysical properties of PAGs.

PAG	$\lambda_{\text{abs}}^{\text{a}}$ , nm	$\epsilon_{\text{max}}^{\text{b}}$ ( $\text{M}^{-1} \text{cm}^{-1}$ )	$\epsilon_{365}^{\text{c}}$ ( $\text{M}^{-1} \text{cm}^{-1}$ )	$T_{\text{d}}^{\text{d}}$
PAG1	313	23803	1003	188
PAG2	313	22835	850	204
PAG3	313	23470	969	167
PAG4	323	4464	392	217
PAG5	322	3776	255	197
PAG6	320	4472	299	160

<sup>a</sup>Wavelength at maximum absorption peak in acetonitrile. <sup>b</sup>Molar extinction coefficients at maximum absorption peak in acetonitrile. <sup>c</sup> Molar extinction coefficients at 365 nm in acetonitrile. <sup>d</sup>Onset temperature of thermal decomposition determined by TGA measurement under atmospheric conditions. Heating rate:  $10 \text{ }^{\circ}\text{C}/\text{min}$ .



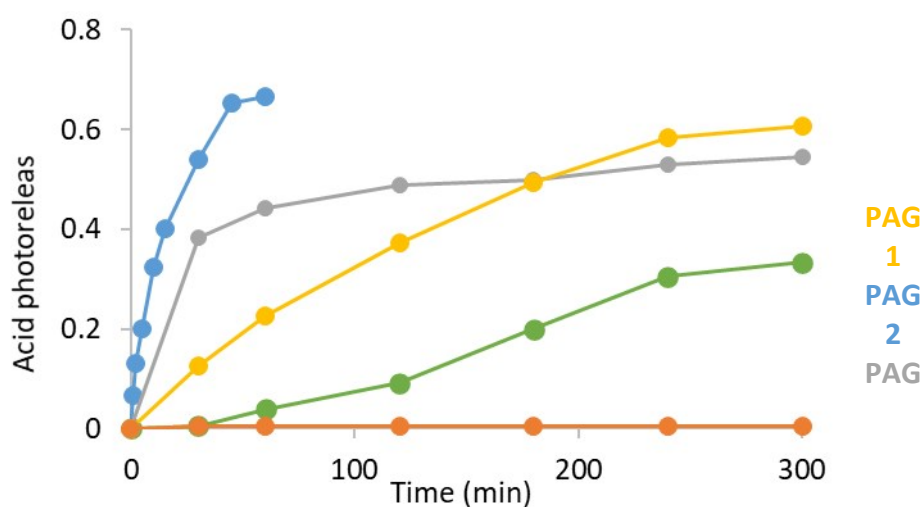


Figure S21: Acid released of PAGs at room temperature as a function of irradiation time in: DMSO- $d_6$  ( $c = 2.5 \cdot 10^{-2}$  M) for PAG1, PAG2, PAG3, PAG4 and PAG5 (yellow, blue, gray, orange and green line respectively),  $CDCl_3$  ( $c = 2.5 \cdot 10^{-2}$  M) for PAG-Im-MSA (Yellow line).

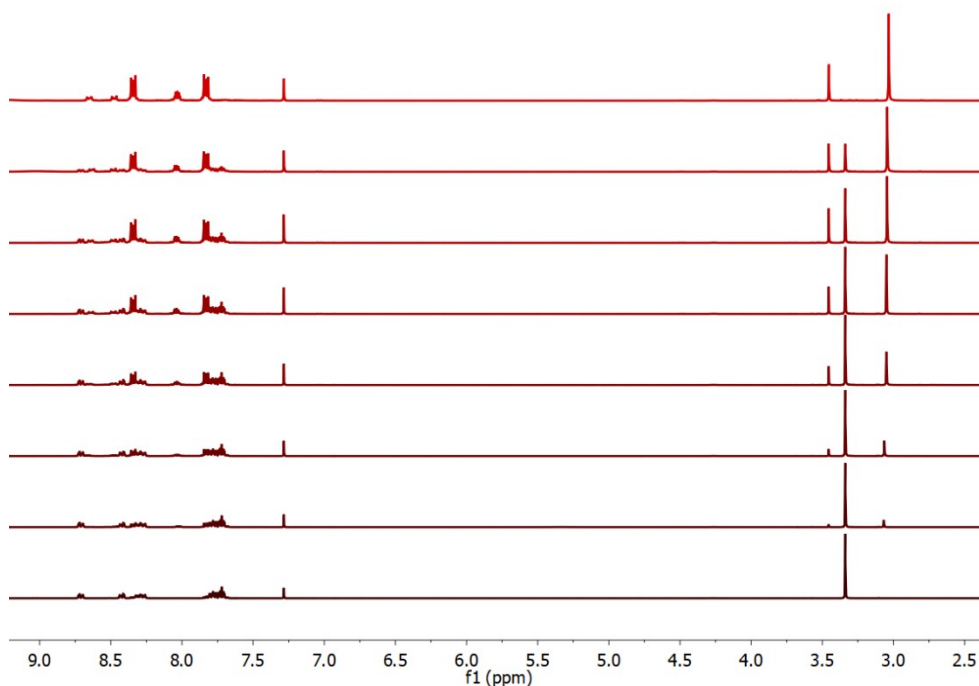


Figure S22:  $^1H$  NMR spectra of a solution containing PAG1 ( $c = 2.5 \cdot 10^{-2}$  M in  $CDCl_3$ ) at room temperature irradiated at different times with a LED source centered at 365 nm (Hamamatsu,  $60 \text{ mW} \cdot \text{cm}^{-2}$ ). Spectra recorded before and after 30, 60, 120, 180, 240, 300 and 360 minutes irradiation (bottom to top).

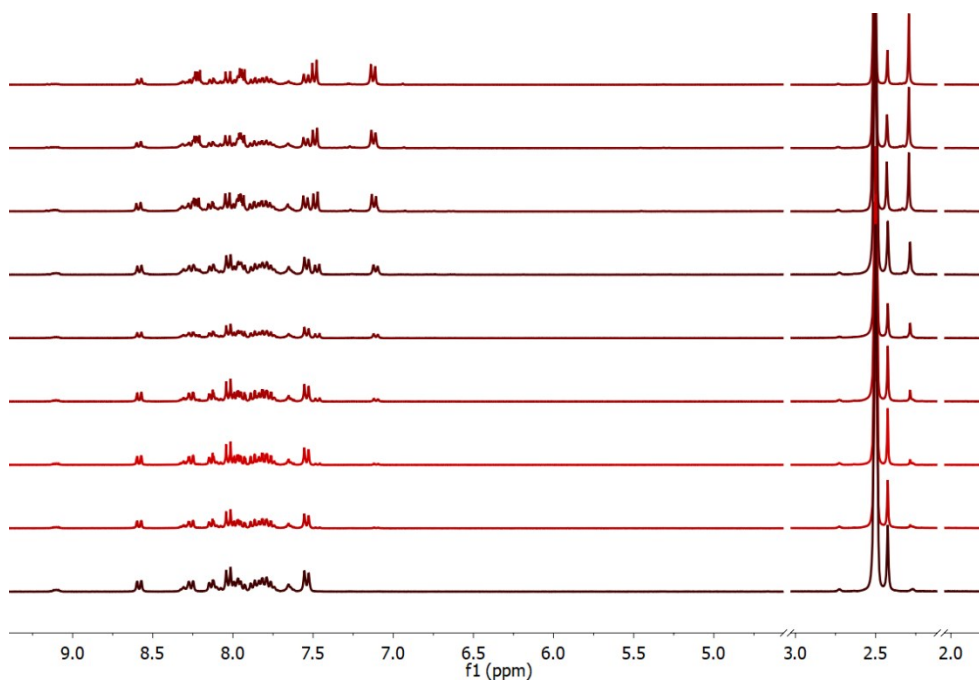


Figure S23:  $^1\text{H}$  NMR spectra of a solution containing PAG2 ( $c = 2.5 \cdot 10^{-2}$  M in  $\text{DMSO-d}_6$ ) at room temperature irradiated at different times with a LED source centered at 365 nm (Hamamatsu,  $60 \text{ mW} \cdot \text{cm}^{-2}$ ). Spectra recorded before and after 1, 2, 5, 10, 15, 30, 45 and 60 minutes irradiation (bottom to top).

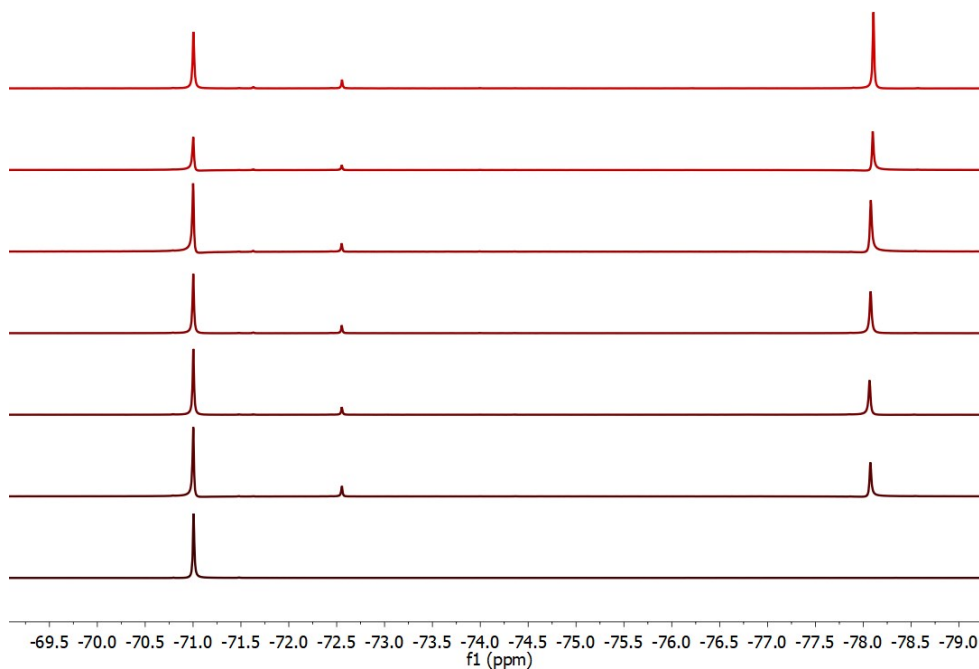


Figure S24:  $^{19}\text{F}$  NMR spectra of a solution containing PAG3 ( $c = 2.5 \cdot 10^{-2}$  M in  $\text{DMSO-d}_6$ ) at room temperature irradiated at different times with a LED source centered at 365 nm (Hamamatsu,  $60 \text{ mW} \cdot \text{cm}^{-2}$ ). Spectra recorded before and after 30, 60, 120, 180, 240 and 300 minutes irradiation (bottom to top).

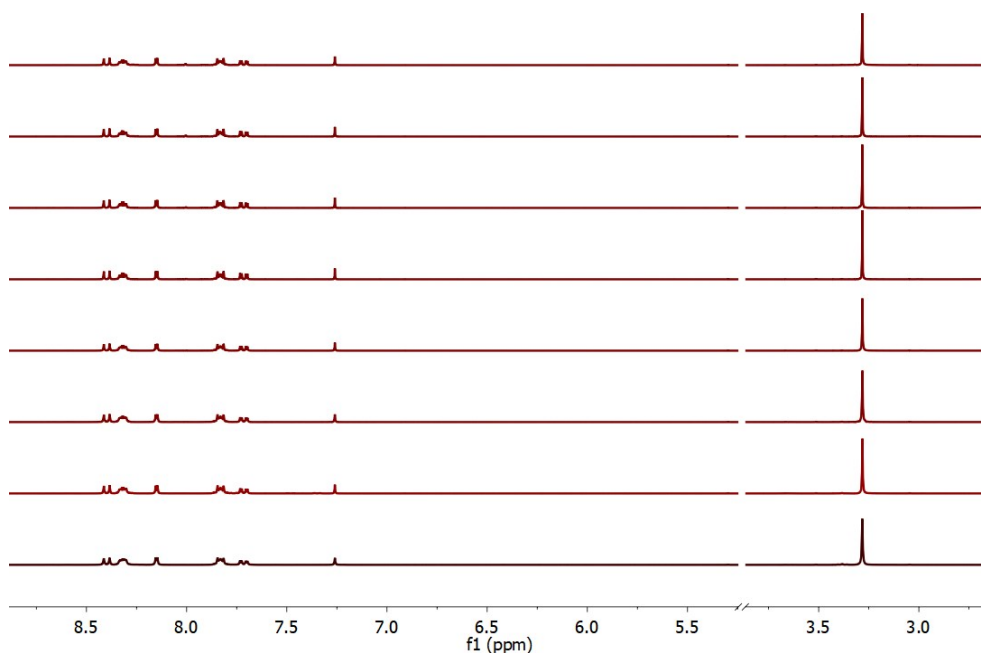


Figure S25:  $^1\text{H}$  NMR spectra of a solution containing PAG4 ( $c = 2.5 \cdot 10^{-2}$  M in  $\text{CDCl}_3$ ) at room temperature irradiated at different times with a LED source centered at 365 nm (Hamamatsu,  $60 \text{ mW} \cdot \text{cm}^{-2}$ ). Spectra recorded before and after 30, 60, 120, 180, 240, 300 and 360 minutes irradiation (bottom to top).

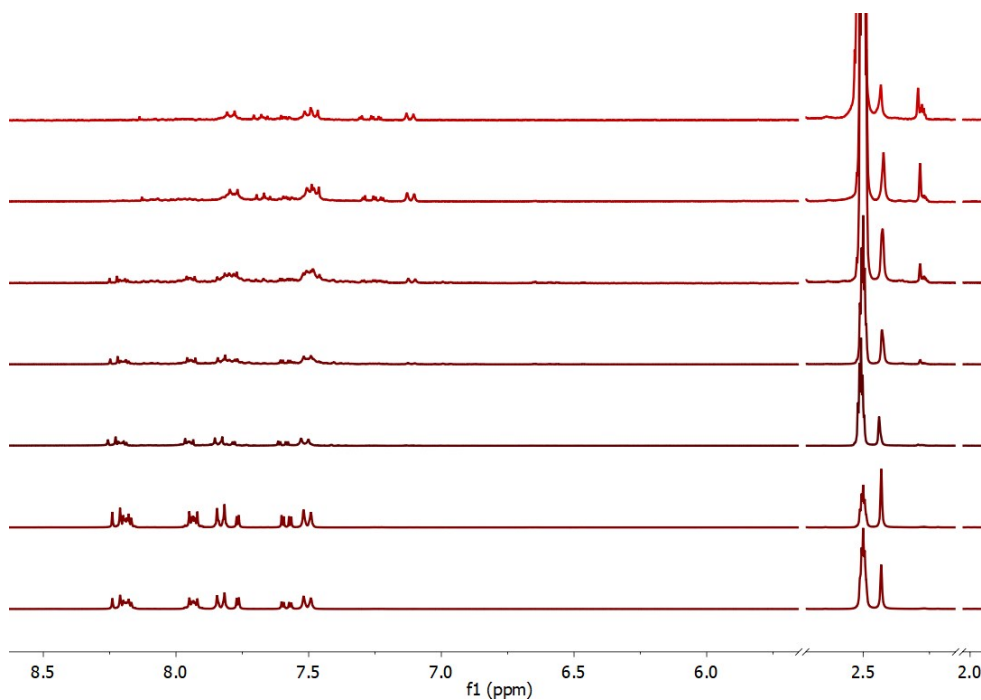


Figure S26:  $^1\text{H}$  NMR spectra of a solution containing PAG5 ( $c = 2.5 \cdot 10^{-2}$  M in  $\text{DMSO-d}_6$ ) at room temperature irradiated at different times with a LED source centered at 365 nm (Hamamatsu,  $60 \text{ mW} \cdot \text{cm}^{-2}$ ). Spectra recorded before and after 30, 60, 120, 180, 240, and 300 minutes irradiation (bottom to top).

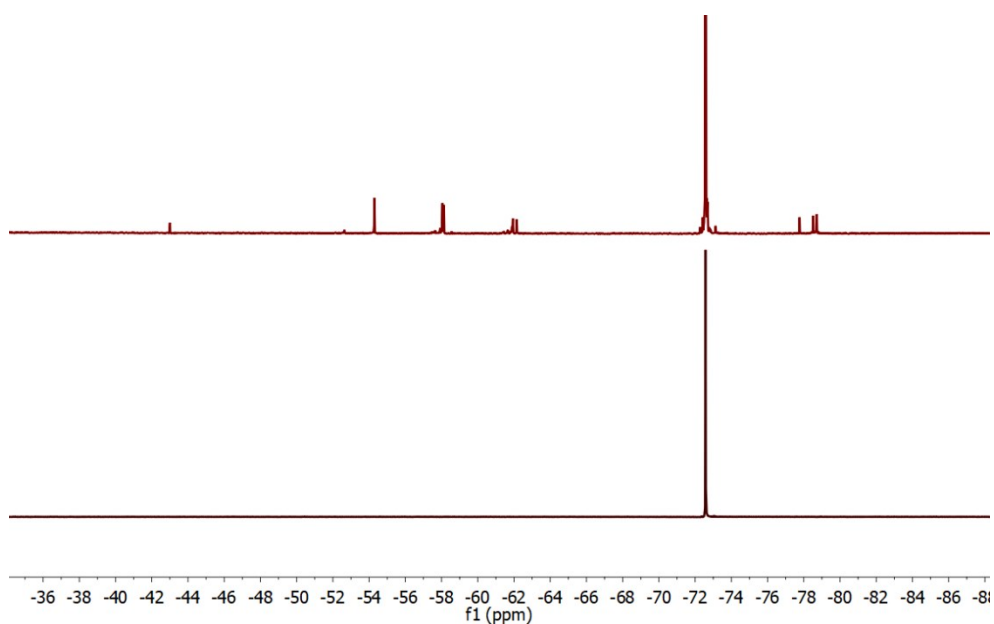


Figure S27:  $^{19}\text{F}$  NMR spectra of a solution containing PAG6 ( $c = 2.5 \cdot 10^{-2}$  M in  $\text{DMSO-d}_6$ ) at room temperature irradiated at different times with a LED source centered at 365 nm (Hamamatsu,  $60 \text{ mW} \cdot \text{cm}^{-2}$ ). Spectra recorded before and after 120 minutes irradiation (bottom to top).

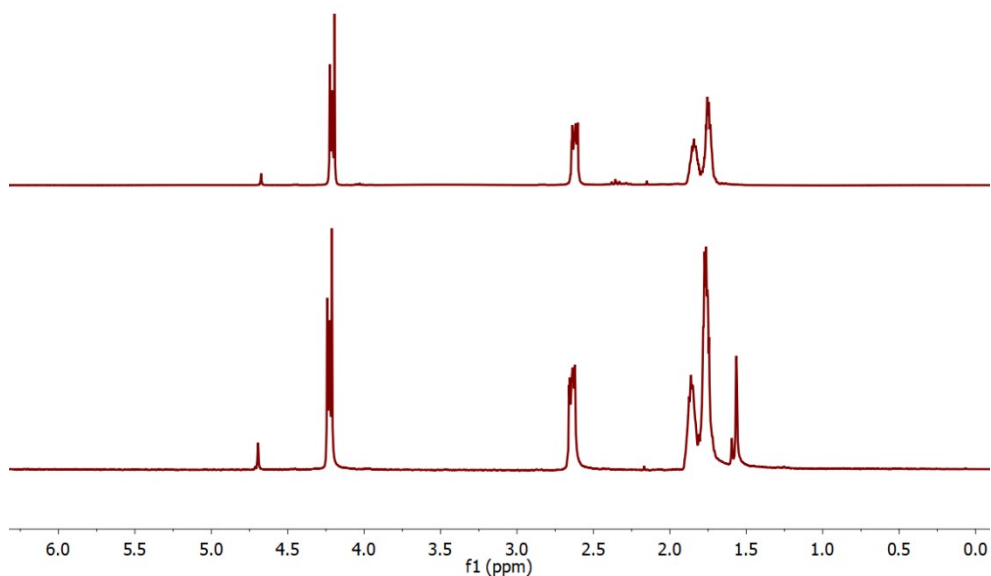


Figure S28:  $^1\text{H}$  NMR spectra in  $\text{CDCl}_3$  of the stability test at room temperature in the darkness containing  $\epsilon\text{-Cl}$ , PAG3 and BnOH. Spectra recorded at  $t_0$  and after 24 h (bottom to top).

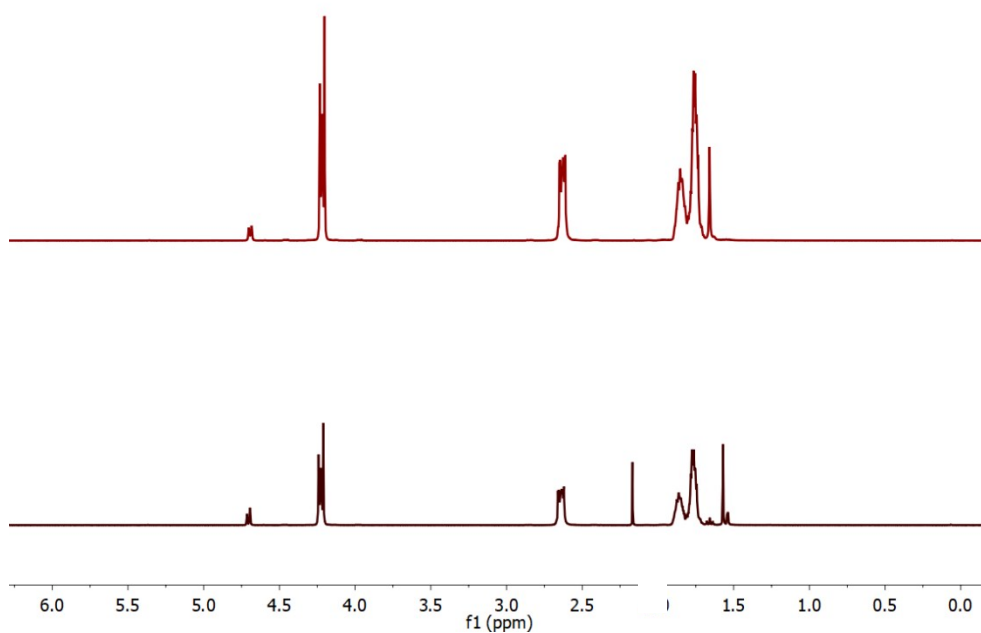


Figure S29:  $^1\text{H}$  NMR spectra in  $\text{CDCl}_3$  of the stability test at room temperature in the darkness containing  $\epsilon\text{-Cl}$ , PAG6 and BnOH. Spectra recorded at  $t_0$  and after 24 h (bottom to top).

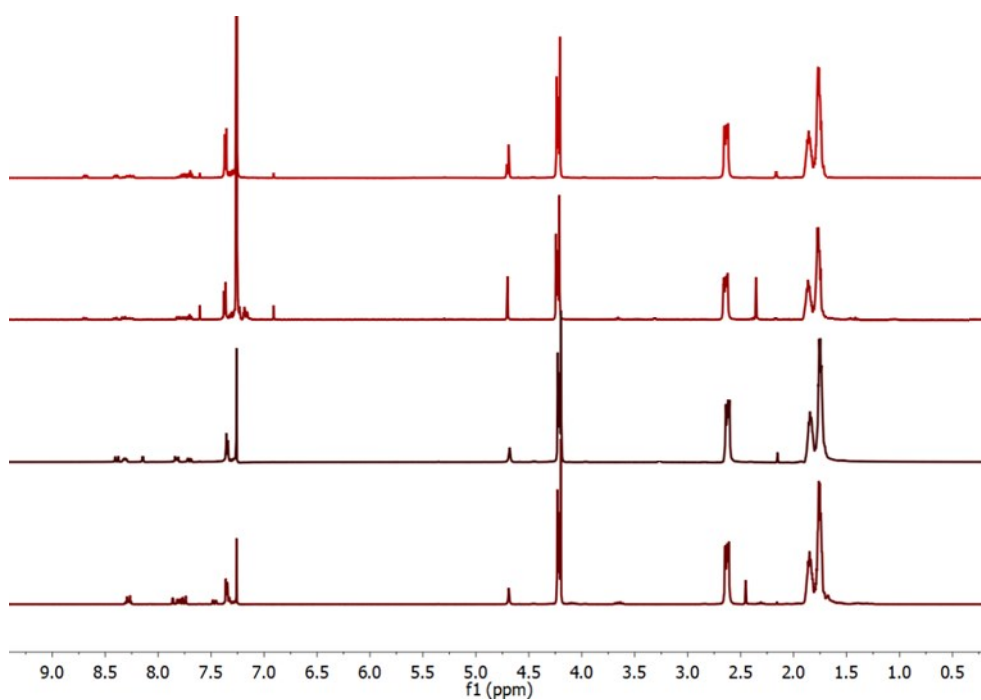


Figure S30:  $^1\text{H}$  NMR spectra in  $\text{CDCl}_3$  of the stability test at  $100\text{ }^\circ\text{C}$  in the darkness containing  $\epsilon\text{-Cl}$ , BnOH and PAG (PAG1, PAG2, PAG4 and PAG5) (bottom to top). Spectra recorded after 3 h.

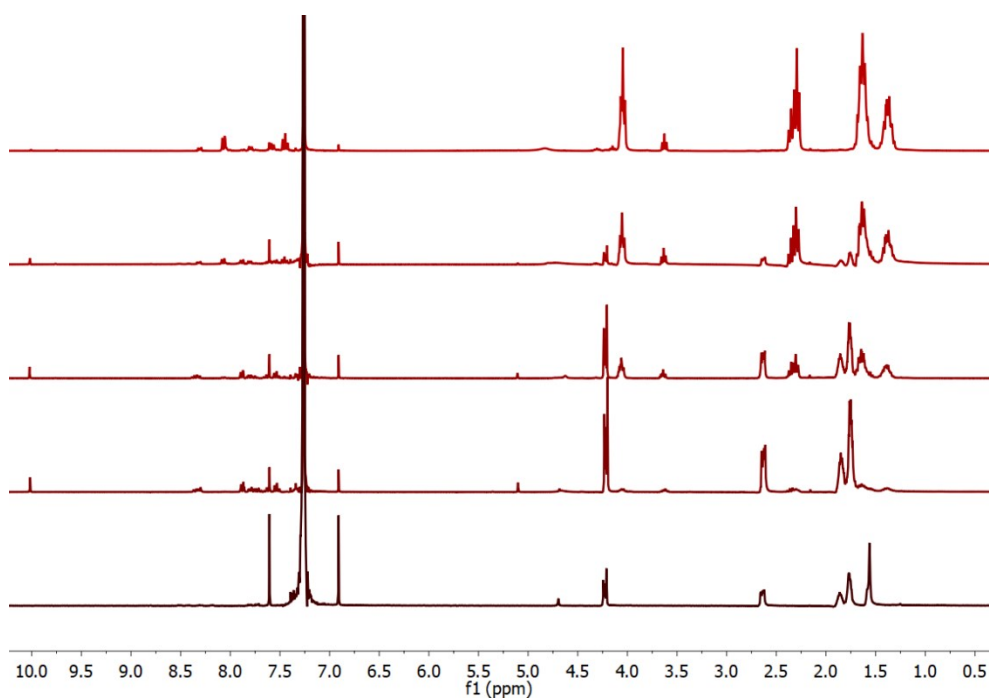


Figure S31:  $^1\text{H}$  NMR spectra in  $\text{CDCl}_3$  of  $\epsilon\text{-Cl}$  polymerization using PAG3 as catalyst and BnOH as initiator irradiated at different times with a LED source centered at 365 nm at room temperature. Spectra recorded before and after 30, 60, 120 and 180 min (bottom to top).

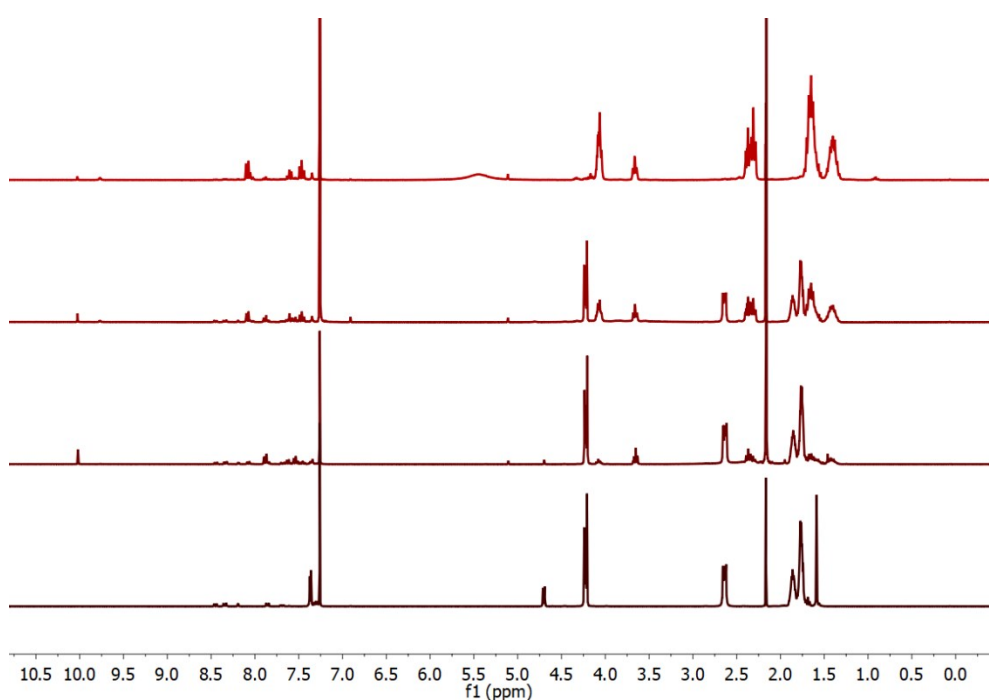


Figure S32:  $^1\text{H}$  NMR spectra in  $\text{CDCl}_3$  of  $\epsilon\text{-Cl}$  polymerization using PAG6 as catalyst and BnOH as initiator (Entry 3) irradiated at different times with a LED source centered at 365 nm at room temperature. Spectra recorded before and after 30, 60, 180 min (bottom to top).

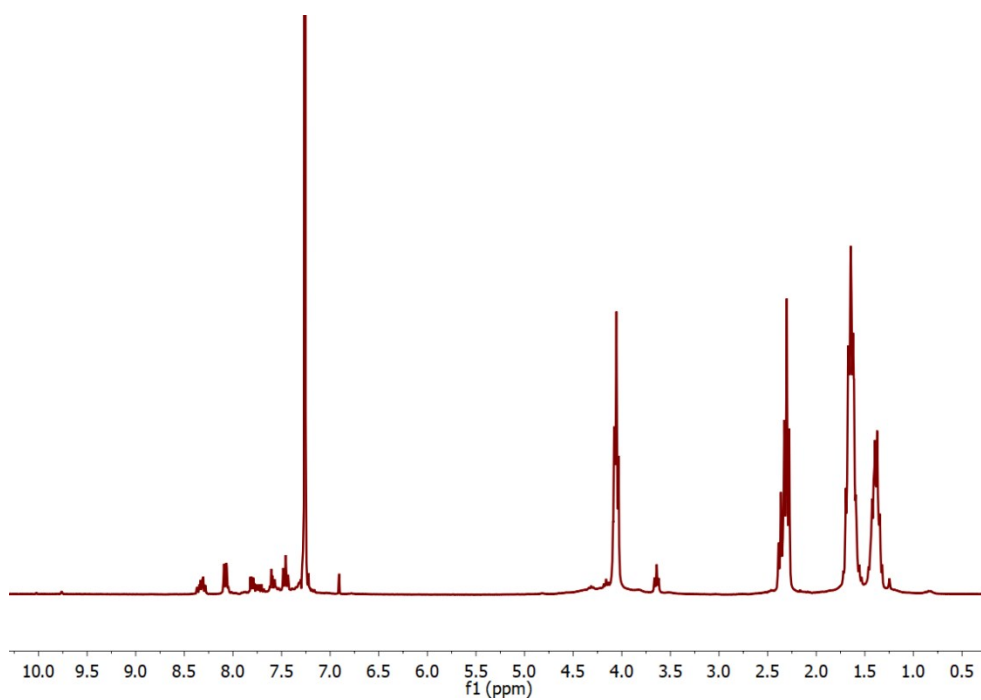


Figure S33: <sup>1</sup>H NMR spectra in CDCl<sub>3</sub> of ε-Cl polymerization using PAG3. and  $[\text{E-Cl}]_0/[\text{BnOH}]_0 = 20$ , Entry 2.

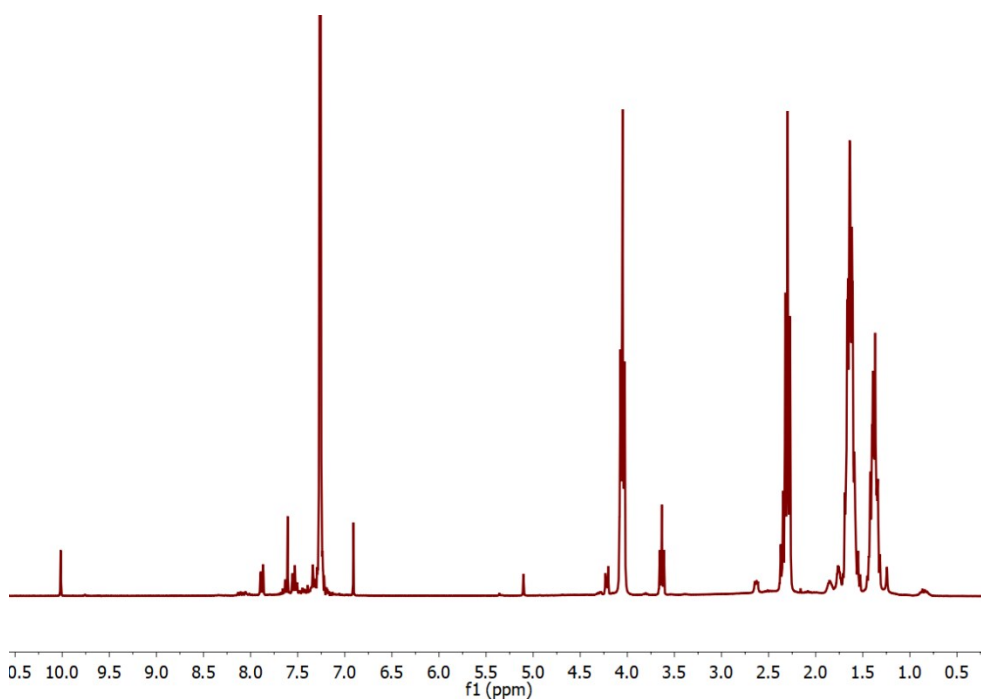


Figure S34: <sup>1</sup>H NMR spectra in CDCl<sub>3</sub> of ε-Cl polymerization using PAG3 . and  $[\text{E-Cl}]_0/[\text{BnOH}]_0 = 50$ , Entry 3

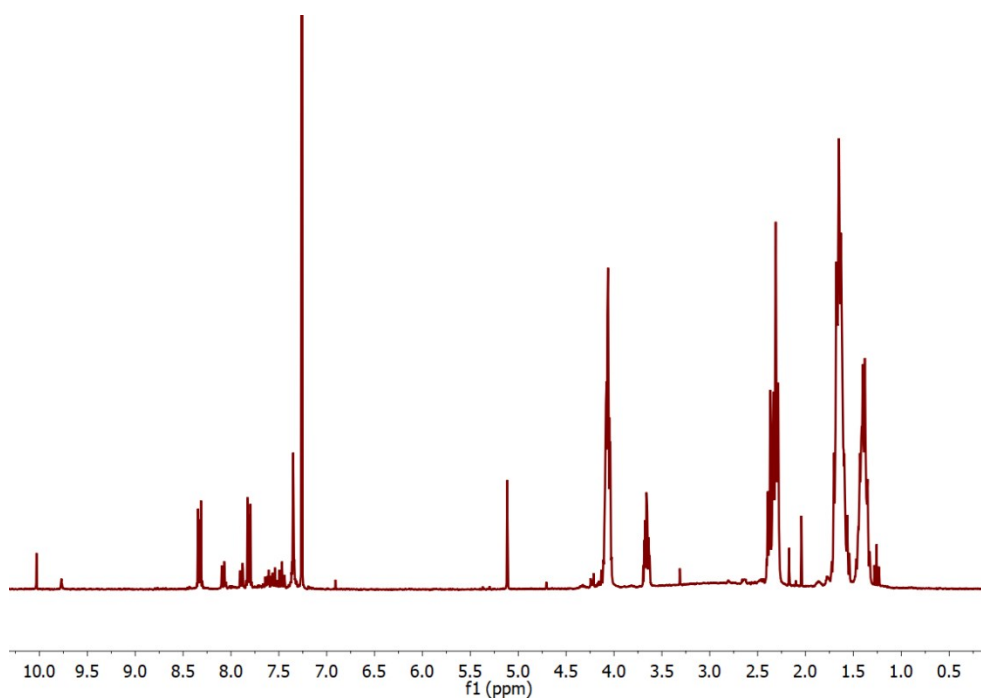


Figure S35: <sup>1</sup>H NMR spectra in CDCl<sub>3</sub> of ε-Cl polymerization after 30 min using PAG2 at 50 °C, Entry 5.

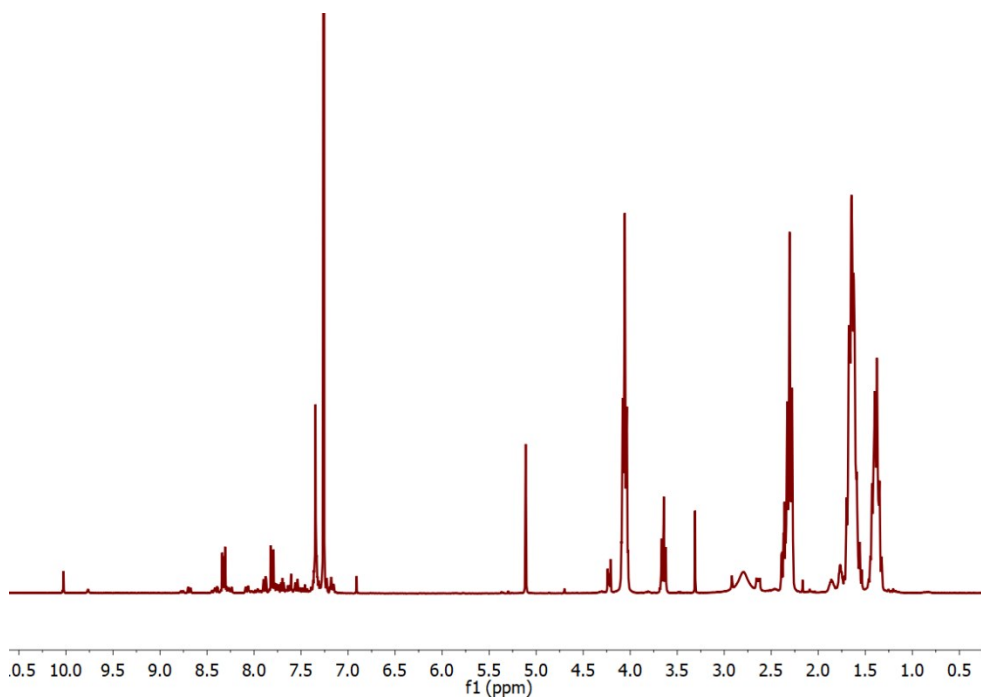


Figure S36: <sup>1</sup>H NMR spectra in CDCl<sub>3</sub> of ε-Cl polymerization after 10 min using PAG2 at 75 °C, Entry 6.



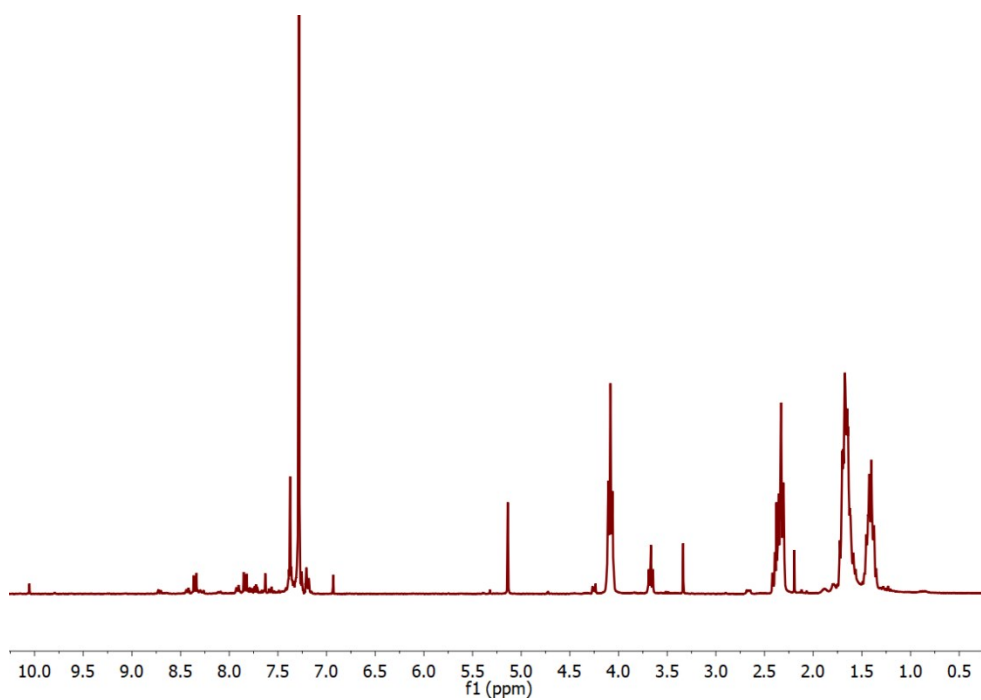


Figure S37: <sup>1</sup>H NMR spectra in CDCl<sub>3</sub> of ε-Cl polymerization after 5 min using PAG2 at 100 °C, Entry 7.

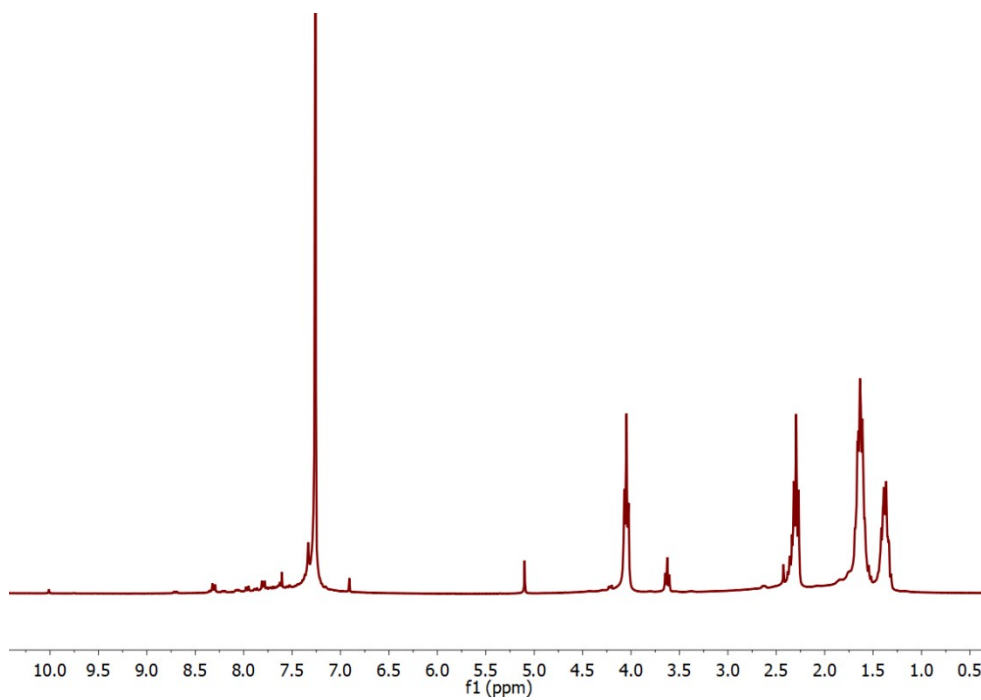


Figure S38: <sup>1</sup>H NMR spectra in CDCl<sub>3</sub> of ε-Cl polymerization after 20 min using PAG1 at 100 °C, Entry 8.

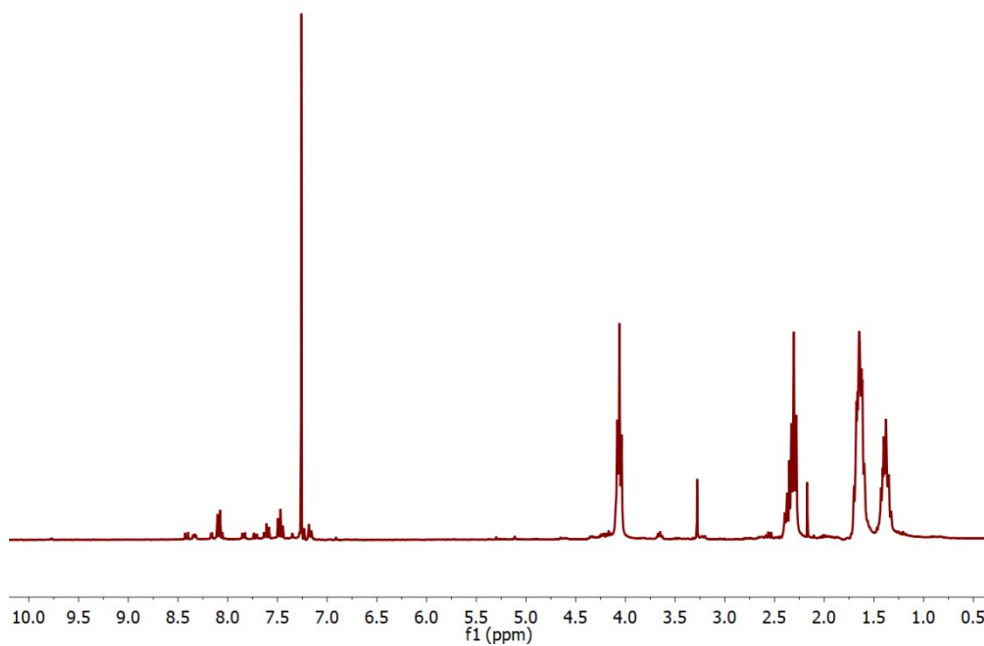


Figure S39: <sup>1</sup>H NMR spectra in CDCl<sub>3</sub> of ε-Cl polymerization after 60 min using PAG4 at 100 °C, Entry 9.

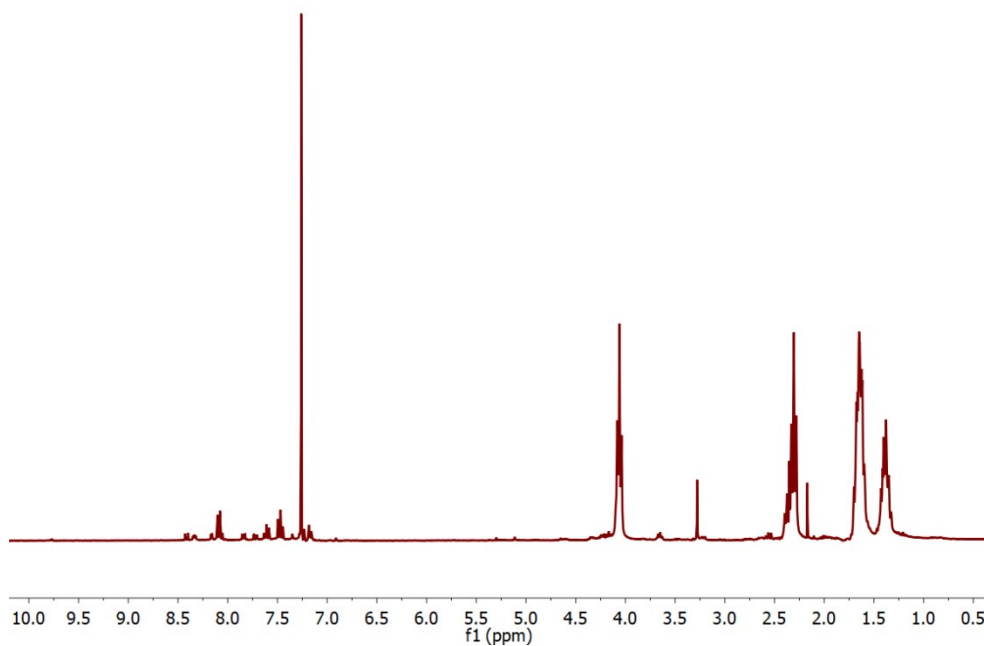


Figure S40: <sup>1</sup>H NMR spectra in CDCl<sub>3</sub> of ε-Cl polymerization after 30 min using PAG5 at 100 °C, Entry 10.

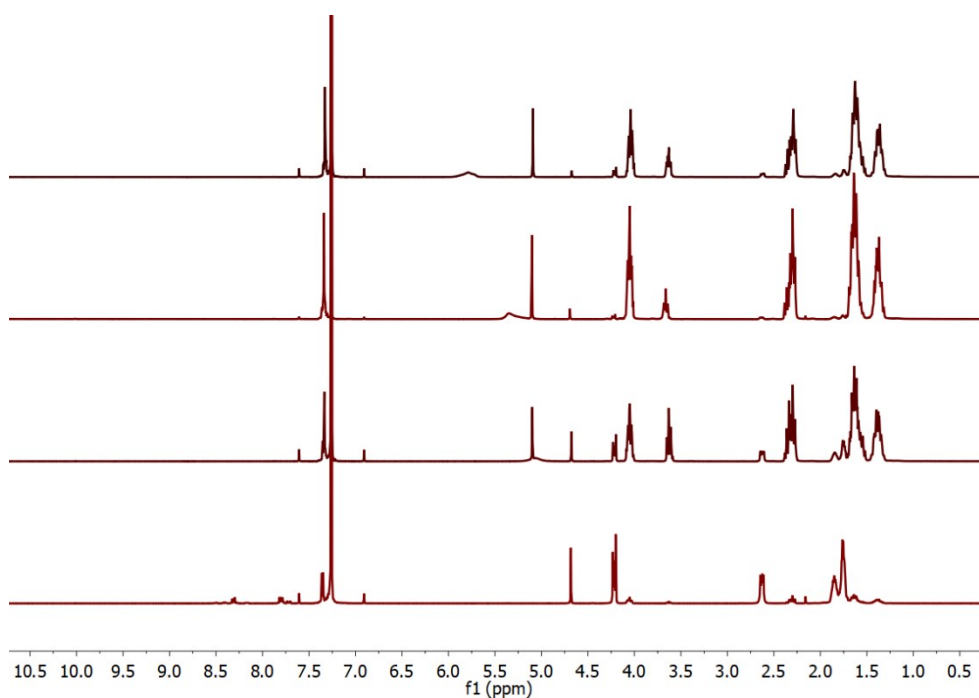


Figure S41: <sup>1</sup>H NMR spectra in CDCl<sub>3</sub> of control ε-Cl polymerization after 30 min using TFSA at room temperature. Spectra recorded before and after 1, 2, and 5 min (bottom to top).

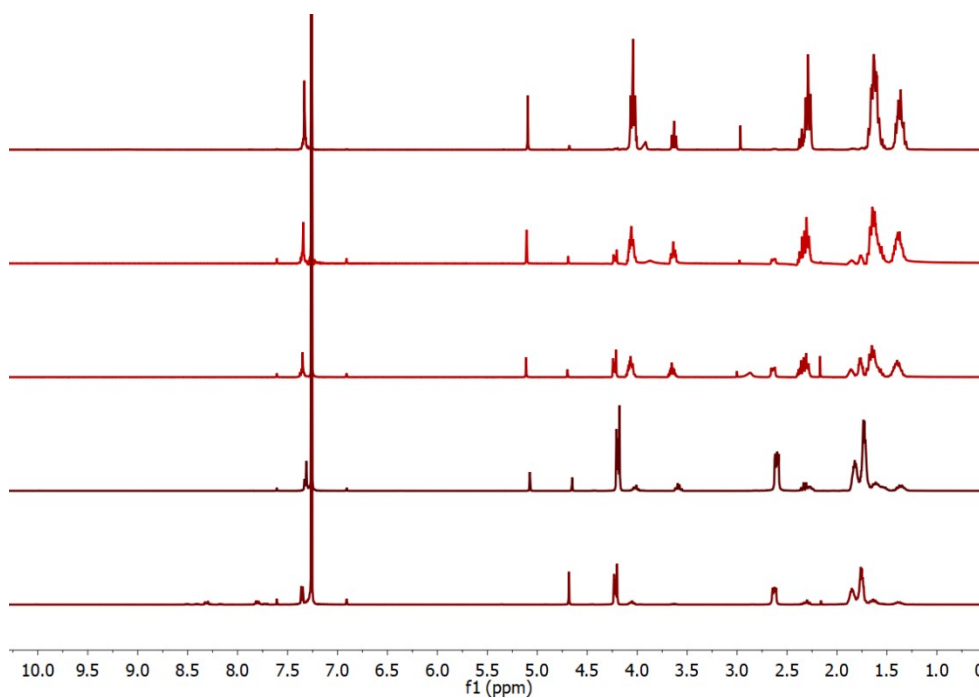


Figure S42: <sup>1</sup>H NMR spectra in CDCl<sub>3</sub> of control ε-Cl polymerization after 30 min using TFSA at room temperature. Spectra recorded before and after 1, 2, 5 and 10 min (bottom to top).

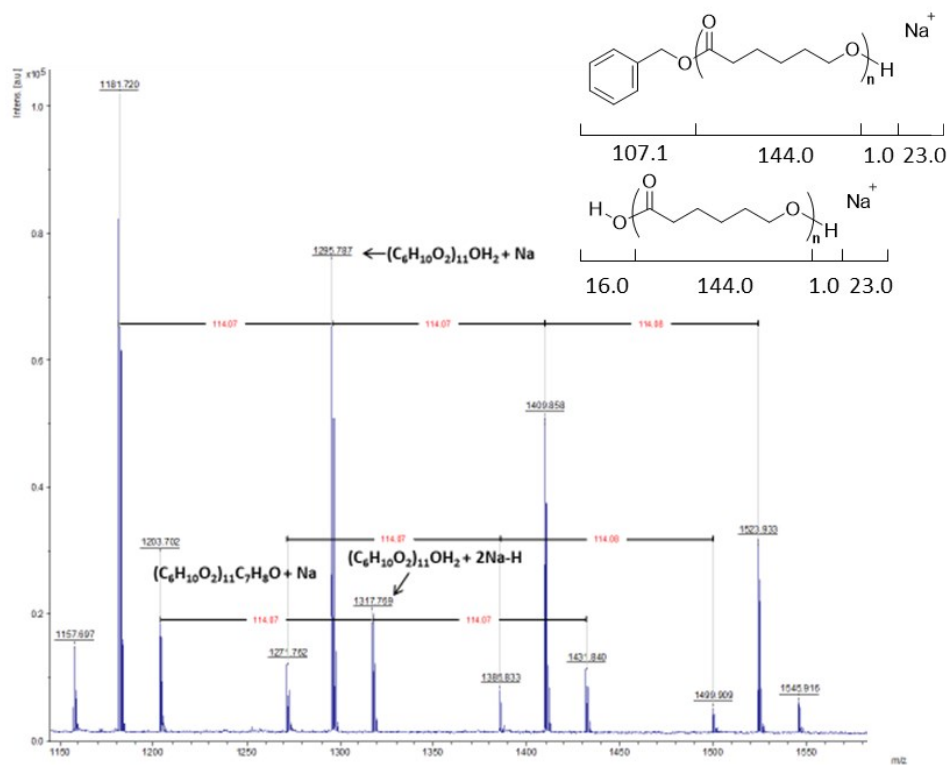


Figure S43: MALDI-ToF MS spectrum of PCL, Entry 1 after 3 h irradiation time.

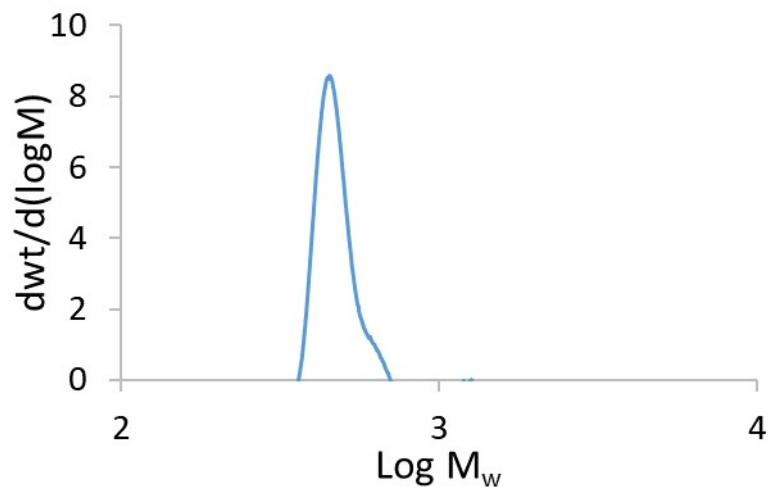


Figure S44: GPC trace of Entry 1 using PAG3 and [E-Cl]<sub>0</sub>/[BnOH]<sub>0</sub> = 10, after 30 min irradiation.

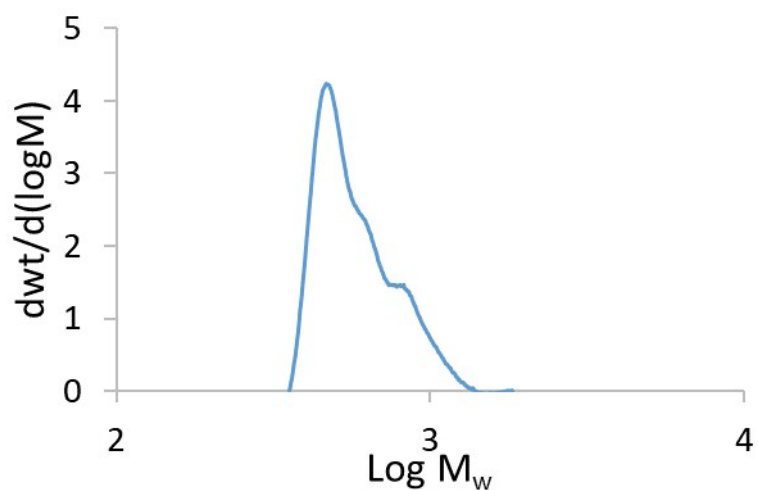


Figure S45: GPC trace of Entry 1 using PAG3 and  $[\epsilon\text{-Cl}]_0/[\text{BnOH}]_0 = 10$ , after 1 h irradiation.

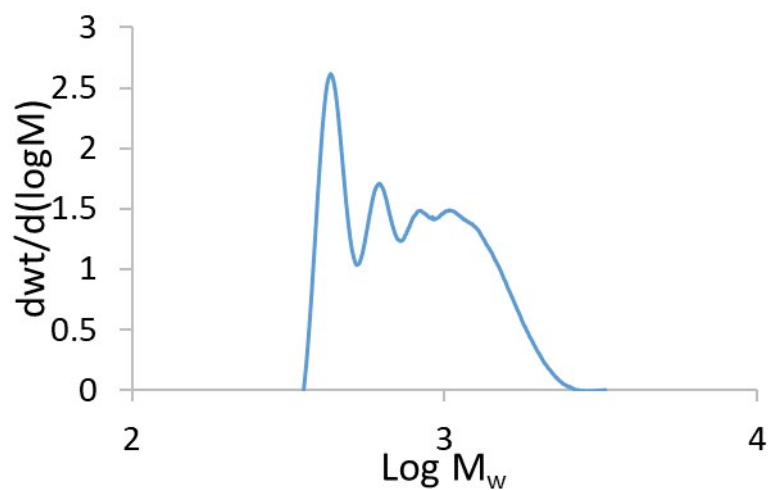


Figure S46: GPC trace of Entry 1 using PAG3 and  $[\epsilon\text{-Cl}]_0/[\text{BnOH}]_0 = 10$ , after 2 h irradiation.

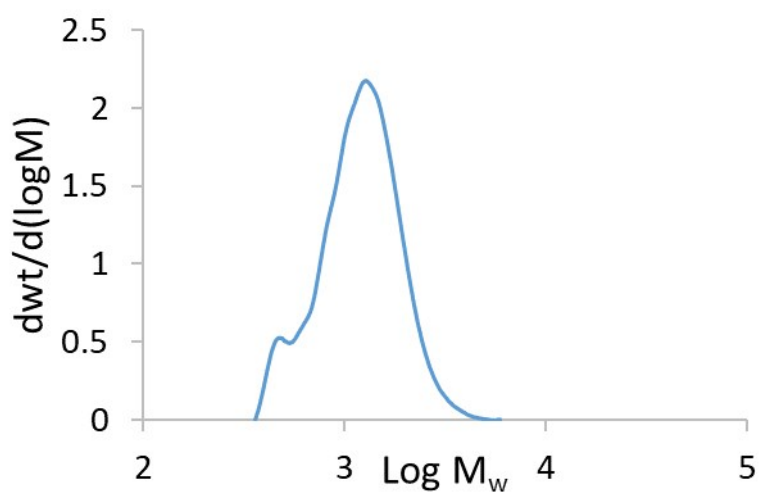


Figure S47: GPC trace of Entry 1 using PAG3 and  $[\epsilon\text{-Cl}]_0/[\text{BnOH}]_0 = 10$ , after 3h irradiation.

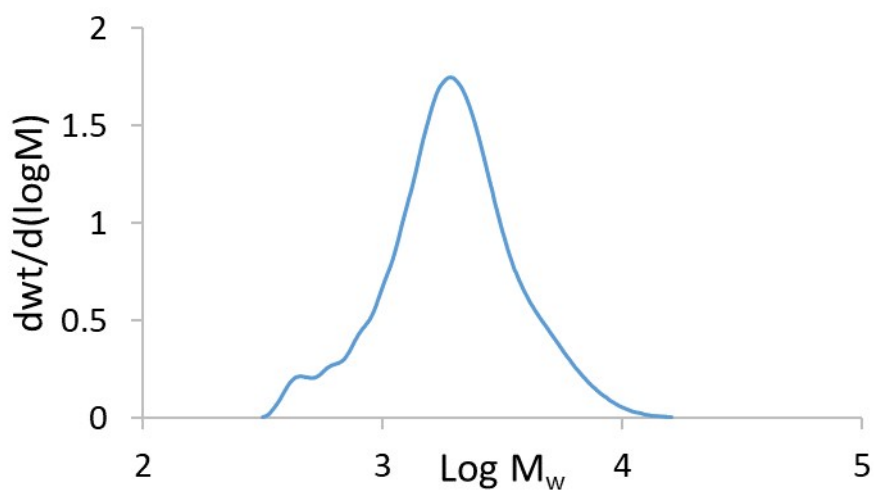


Figure S48: GPC trace of Entry 2 using PAG3 and  $[\text{E-Cl}]_0/[\text{BnOH}]_0 = 20$ , after 3 h irradiation.

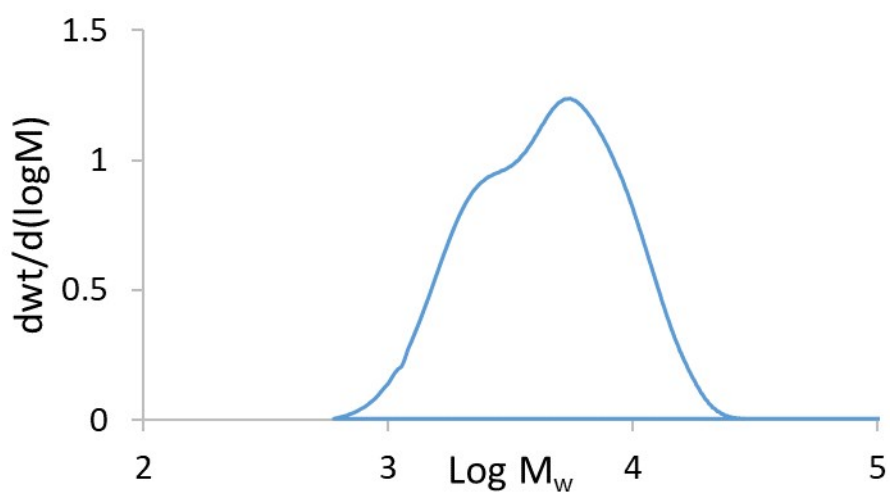


Figure S49: GPC trace of Entry 3 using PAG3 and  $[\text{E-Cl}]_0/[\text{BnOH}]_0 = 50$  after 6 h irradiation.

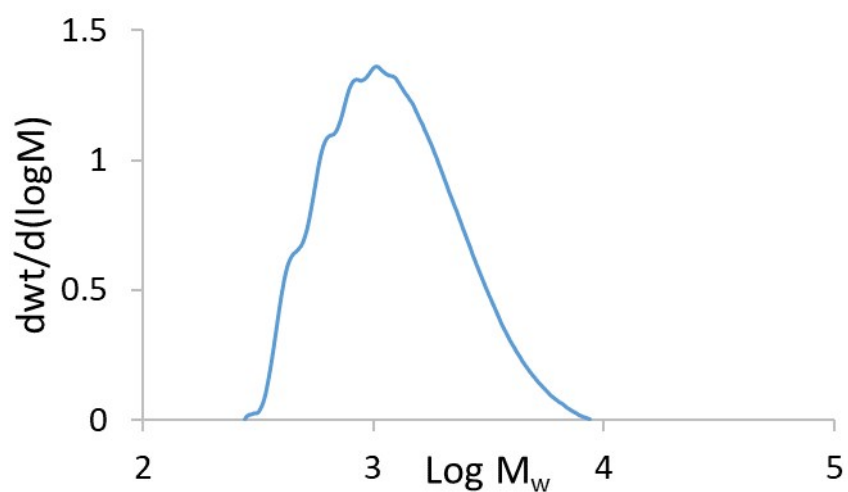


Figure S50: GPC trace of Entry 4 using PAG6 and  $[\text{E-Cl}]_0/[\text{BnOH}]_0 = 10$ , after 3 h irradiation.

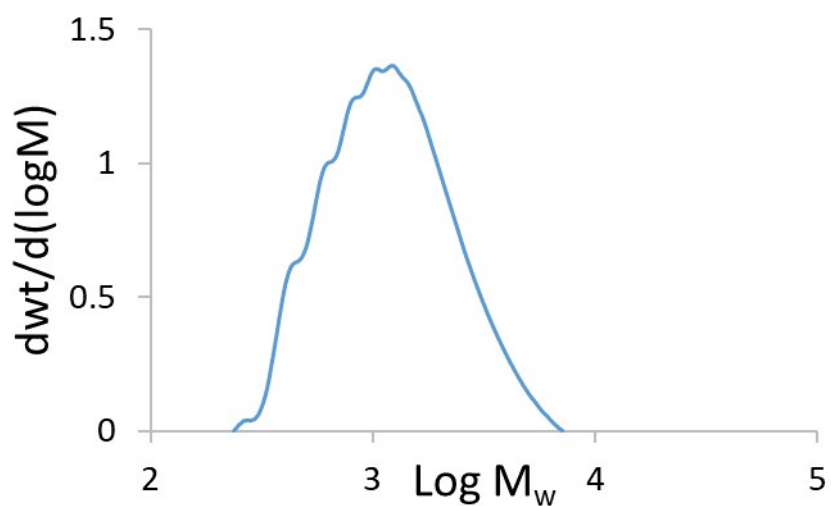


Figure S51: GPC trace of Entry 5 using PAG2 at 50 °C, after 30 min irradiation.

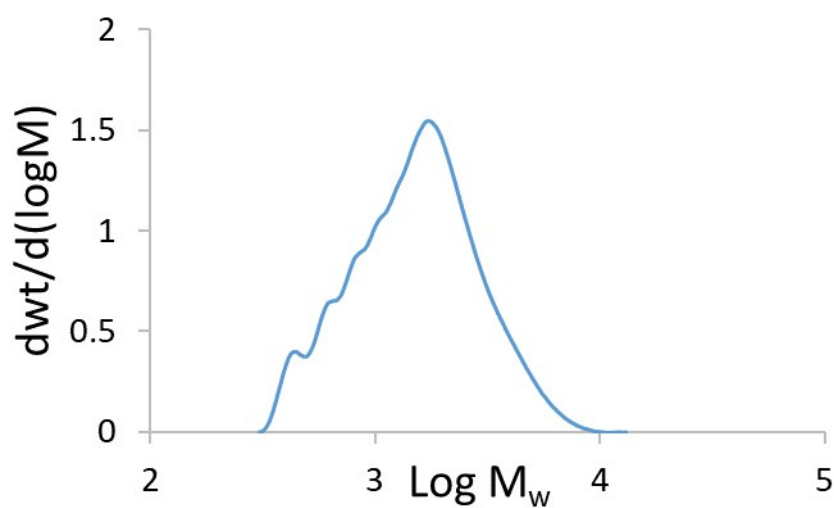


Figure S52: GPC trace of Entry 6 using PAG2 at 75 °C, after 10 min irradiation.

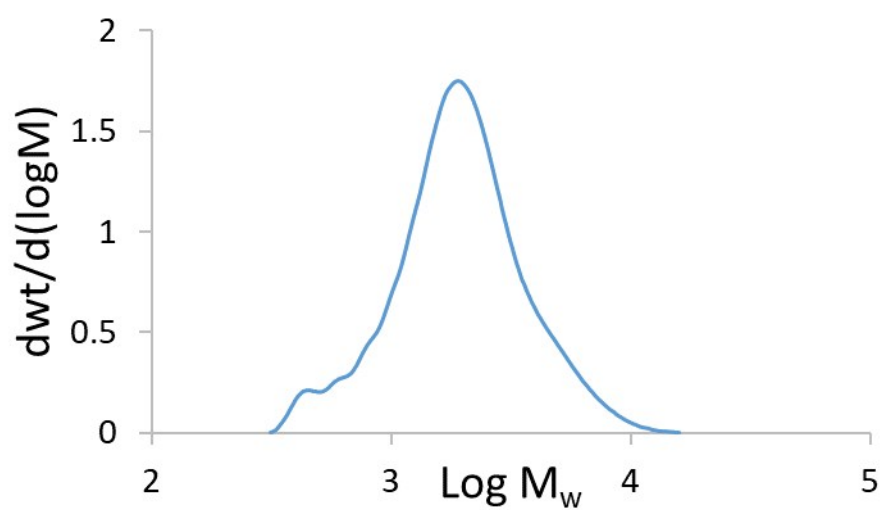


Figure S53: GPC trace of Entry 7 using PAG2 at 100 °C, after 5 min irradiation.

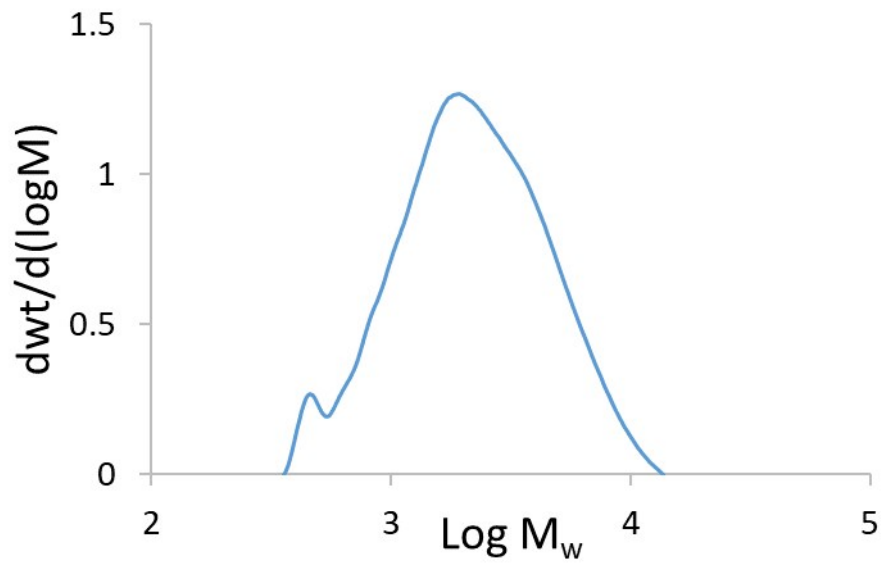


Figure S54: GPC trace of Entry 8 using PAG1 at 100 °C, after 20 min irradiation.

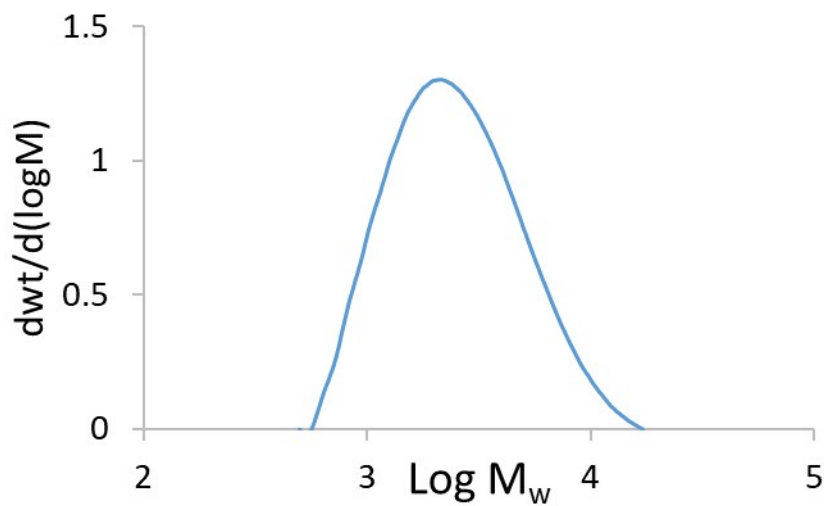


Figure S55: GPC trace of Entry 9 using PAG4 at 100 °C, after 60 min irradiation.

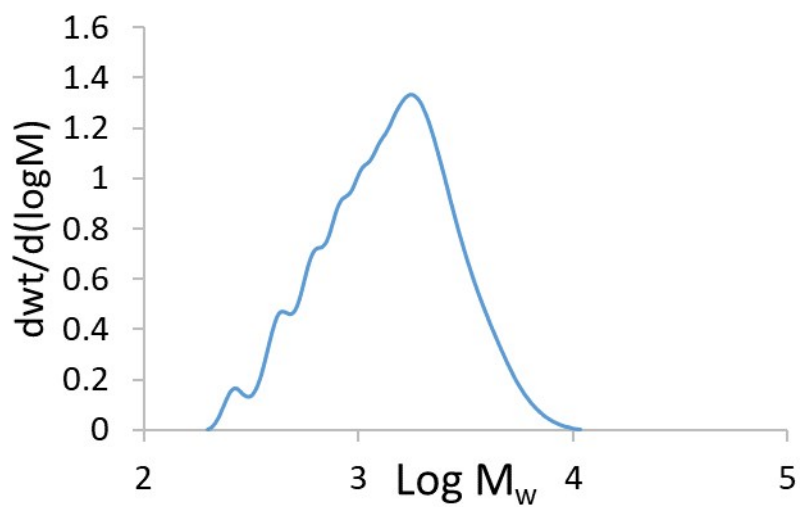


Figure S56: GPC trace of Entry 10 using PAG5 at 100 °C, after 30 min irradiation.



#### 4. Supplementary methods

**Nuclear Magnetic Resonance (NMR) Spectroscopy.**  $^1\text{H}$  NMR and  $^{13}\text{C}$  NMR were performed at room temperature with a Bruker Avance DPX 300:  $^1\text{H}$  (300 MHz) and  $^{13}\text{C}$  (75 MHz).  $^{19}\text{F}$  NMR were recorded at room temperature with a Bruker AC-400 spectrometer. The  $^1\text{H}$  chemical shifts were reported in parts per million (ppm) and were referenced to the solvent peak DMSO (2.50 ppm) and  $\text{CDCl}_3$  (7.26 ppm). The  $^{13}\text{C}$  chemical shifts were determined by  $^{13}\text{C}$ -APT experiment. They were reported in ppm and were referenced to the solvent peak DMSO (39.5 ppm) and  $\text{CDCl}_3$  (77 ppm).

**Mass Spectroscopy.** Mass spectra were recorded by ultrahigh performance liquid chromatography (UPLC, Acquity system from Waters Chromatography S.A., USA) coupled to a high-resolution mass spectrometer (Synapt G2 from Waters Chromatography S.A., USA, time-of-flight analyzer (TOF)) by an electrospray ionization source in positive mode (ESI).

**Thermal Stability Experiments.** Thermogravimetric analysis (TGA) was performed in the Netzsch (STA449-F3). The temperature range was from room temperature to 600 °C, and the heating rate was 20 °C  $\text{min}^{-1}$  under ambient conditions.

**UV-VIS:** Absorbance measurements were recorded in an Agilent 8453 UV-Visible spectrophotometer.

**Rheological measurements:** An AR-G2 rheometer (TA Instruments) equipped with disposable aluminum plates of 12 mm was used to perform dynamic frequency sweep experiments from 0.01 to 100 Hz at 30 °C. The strain used during the experiments was fixed to 1 %.

**MALDI-TOF MS:** A Bruker Autoflex Speed system (Bruker, Germany) equipped with a Smartbeam-II laser (Nd:YAG, 355 nm, 2 kHz) was used. Spectra were acquired in reflection mode; each mass spectrum was the average of 8000 shots. Samples were dissolved in THF at a concentration of 10  $\text{mg}\cdot\text{mL}^{-1}$ . *trans*-2-[3-(4-*tert*-Butylphenyl)-2-methyl-2-propenylidene] malononitrile (DCTB, Sigma-Aldrich) was used as a matrix. The matrix was dissolved in THF at a concentration of 20  $\text{mg}\cdot\text{mL}^{-1}$ . Sodium trifluoroacetate (NaTFA) (Fluka) was used as cation donor (10  $\text{mg}\cdot\text{mL}^{-1}$  dissolved in THF). The samples were mixed with the matrix and salt at a 10 : 2 : 1 (matrix/sample/salt) ratio. Approximately 1  $\mu\text{L}$  of the obtained mixture was hand spotted on the ground steel target plate.

**Gel content (GC).** Two specimens from the same sample, each weighing  $\sim 0.15$  g were introduced in a Soxhlet extraction sleeve and extracted for 24 h in refluxing tetrahydrofuran. After this treatment, the non-crosslinked fraction is supposed to be dissolved in the solvent and thus could be separated from the crosslinked insoluble fraction (gel). This crosslinked residue was dried in the oven at 65 °C for 24 h followed by the determination of its weight. The ratio between the insoluble fraction and the initial mass of the sample gives the gel content:

$$\text{Gel content (\%)} = \frac{\text{Insoluble residue mass}}{\text{Initial mass}} \times 100$$

#### Materials

All reagents and solvents were purchased from Sigma-Aldrich, TCI Chemicals or Fisher and they were used without further purification unless otherwise specified.

## 5. References

1. Surkau, G., Böhm, K. J., Müller, K. & Prinz, H. Synthesis, antiproliferative activity and inhibition of tubulin polymerization by anthracenone-based oxime derivatives. *Eur. J. Med. Chem.* **45**, 3354-3364 (2010).
2. Pal, J., Kankariya, N., Sanwaria, S., Nandan, B. & Srivastava, R. K. Control on molecular weight reduction of poly( $\epsilon$ -caprolactone) during melt spinning - A way to produce high strength biodegradable fibers. *Mater. Sci. Eng. C* **33**, 4213-4220 (2013).